 # Referee 1

This is an excellent paper. It clearly demonstrates the need to include ocean wind wave effects as part of a sea ice modelling framework. The paper does not attempt to include all possible wave effects, for all situations, but rather, it limits itself to the role of the momentum flux due to waves attenuation by sea ice and the role of wave-induced sea ice break-up in lateral melt. There are many more steps towards the full inclusion of ocean waves into the sea ice modelling framework but this is a good first step.

We thank the reviewer for their careful reading of our manuscript and for their comments and suggestions. We have tried to address their questions and concerns, as detailed in the following. In our comments, PXLY refers to page X line Y of the attached updated manuscript.

Minor corrections:

Page 1, line 22: consider adding Waseda et al. 2018 to Thomson and Rogers 2014
Waseda et al. (2018): Correlated Increase of High Ocean Waves and Winds in theIce-Free Waters of the Arctic Ocean. Scientific Reports, 8, Article number: 4489https://www.nature.com/articles/s41598-018-22500-9
We have added these references (P2L3).

Page 2, line 4: consider adding Bateson et al. (2019) Adam W. Bateson et al, 2019: Impact of floe size distribution on seasonal fragmentation and melt of Arctic sea ice. https://www.the-cryosphere-discuss.net/tc-2019-44
We have added the reference later in the text, but did so in some other places where it seemed more relevant to us (P3L8, P14L13...).

Page 4, line 27: some fetch for the generation of sea ice. It is what you mean or rather some fetch for the generation of sea waves (?)
It was indeed a typo and we have fixed it.

Page 5, (1). I assume that Sice is defined as being positive, hence in WW3, it appears as –Sice. Just clarify.
Our definition of Sice has been clarified in the updated manuscript (P6L14).

Page 6, line9: panels b,e→panels b,d
Fixed
Page 10, line 19 : there is no figure 5 e nor (line 21), 5 f
Fixed

 # Referee 2

Coupling a sea ice and an ocean surface wave model is a valuable step forward, enabling investigation of marginal ice zone physics as well as potential advances for both sea ice and wave forecasting. The results on the impact of wave radiation stress on sea ice are very interesting, and certainly worth publication. In fact, the novelty of including this process in a commonly-used, pan-Arctic sea ice model should be emphasized further in the text. However, the manuscript includes some unclear reasoning and the floe size distribution model developed to examine the impact of lateral melt raises some questions that I list below in 'Specific Comments'. I also noted some incorrect representation of the literature. In general, the manuscript is hard to follow, uses inaccurate or informal phrasing in places and contains a number of grammatical and typographical errors. It requires a thorough proof-read before resubmission. I have listed some sentences to be rephrased at the end of the review, but note that this is not an exhaustive list. When re-writing, the authors should carefully check where the text can be made clearer and more concise.

We thank the reviewer for their careful reading of our manuscript and for their comments and suggestions. We have tried our best to address their questions and concerns, as detailed in the following. A careful proof-reading of the text has been done to improve the readability of the text. In our comments, PXLY refers to page X line Y of the attached updated manuscript.

Specific Comments:

P1 L2 and P1 L20: Strong et Rigor (2013) find that the Arctic MIZ (defined by sea ice concentration) has been expanding in summer and contracting in winter over the recent historical period. This should be referenced in the text.

We now refer to Strong et Rigor (2013) in the introduction (P2L2)

P1 L2: 'Yet, state-of-the-art models are not capturing the complexity of the varied processes occurring in the MIZ, and in particular the processes involved in the ocean-sea ice interactions.' This is a very broad and vague sentence. The models may not include certain processes that occur in the MIZ, but they may be able to capture their large-scale impacts through parametrizations.

The sentence has been changed to:

P1L2: "*Yet, state-of-the-art models exhibit significant biases in their representation of the complex ocean-sea ice interactions taking place in the MIZ."*

P1 L15-19: I would suggest the authors be more specific here about what processes they are referring to

We have added a few examples:

P1L5*: "Indeed, the MIZ is characterized by a wide variety of processes resulting from the highly non-linear interactions between the atmosphere, ocean and sea ice: sea ice floe fragmentation and welding, lead opening and associated heat transfers, mesoscale and submesoscale features arising from strong temperature and salinity gradients (see Lee et al., 2012, for a review and references therein)..."*

P2 L20: Check the location of reference placement in these sentences.

This has been fixed.

P2 L31: I would dispute the phrasing that 'In contrast, little progress has been done regarding the inclusion of waves in coupled ocean-sea ice models.' Simulation of the FSD within a climate-scale sea ice model is the first step required to model fracture of sea ice by ocean surface waves, and the past few years have seen much progress in this area: Zhang et al. (2015,2016), Horvat et Tziperman (2015), Bennetts et al. (2017), Roach et al. (2018), Bateson et al. (2019, in review). These studies have used simple representations of waves in order to develop the physics relating to sea ice, just as the studies focusing on the impact of sea ice on waves (Dumont et al. 2011, Williams et al. 2013, etc) have prescribed sea ice conditions and/or neglected certain sea ice physics. These paragraphs should be rewritten to more accurately reflect the current state of the literature, including all references I listed above. Additionally, I would use 'simple' rather than 'crude', which has negative connotations.

We agree with the reviewer that this paragraph was too negative considering the amount of work recently done on FSDs in sea ice models. We therefore rephrased it to emphasize the step-by-step progress that have allowed us to perform this study. We also added missing references to the work of Roach et al. (2018) and Bateson et al. (2019).

P3L1: *"In parallel, progress has also been made regarding the inclusion of the effects of waves in coupled ocean-sea ice models. Using a very simple parameterization, Steele et al. (1989) and Perrie and Hu (1997) have investigated the effect of WRS on sea ice drift in the MIZ, only considering the attenuation of waves generated between the ice floes, and found a limited impact on the sea ice conditions. More recently, Williams et al. (2017) implemented a wave module in the semi-Lagrangian sea ice model neXtSIM (Rampal et al., 2016) and found that high wave conditions can cause a significant displacement of the sea ice edge. The implementation of FSDs in different sea ice models, as introduced by Zhang et al. (2015) and Horvat and Tziperman (2015) for instance, has also opened the way to the assessment of the potential enhancement of lateral melt by wave-induced ice fragmentation (Zhang et al., 2016; Bennetts et al., 2017; Roach et al., 2018; Bateson et al., 2019), but the representation of waves remains too simple to simulate the full effect of waves on the evolution of sea ice."*

P3 L16: It would be useful to include a brief summary of the different processes by which sea ice affects waves in the model, for readers not familiar with the Boutin et al. (2018) paper.

We have added the following sentence in section 2 to briefly describe the model detailed in Boutin et al. (2018):

P3L27: "*These processes are scattering (which redistributes the wave energy without dissipation), friction under sea ice (with a viscous and a turbulent part depending on the wave Reynolds number), and inelastic flexion. All these processes depend on sea ice thickness and concentration, and scattering and inelastic flexion also depend on floe size."*

P4 L1: What does 'Arctic realistic simulation' mean?

This sentence has been fully rephrased:

P4L17: *"The wave spectrum used as forcing at the boundary is extracted at a point south of Svalbard from an Arctic hindcast performed with WW3 described by Stopa et al. (2016). It covers the period of May 2nd to 3rd, 2010, during which a storm occurred in this particular area (Collins et al. 2015)."*

P4 L24: Describe the Lupkes et al. (2012) parametrization at its first mention, or don't mention it here.
We have removed this reference and modified the sentence as follows:
P5L7:"[...], in which the already existing lateral melt parameterization in LIM3 is activated."

P4 L23: If I understand correctly, the full NEMO ocean model is initialized from a climatology and spun-up for nine years. This seems to be a rather short spin-up period. How was it determined that nine years was sufficient? Similarly, how was it determined that three days was a sufficient adjustment period for the introduction of the wave coupling?
Regarding the ocean-sea ice model, the spin up would indeed be too short to allow for a full adjustment of the full water column. However, here, we only focus on ocean surface processes, that are expected to quickly respond to the atmospheric and sea ice forcing, for which 9 years is largely enough to equilibrate. Regarding waves, a spin up of a few days is what we typically use in all WW3 simulations.
We also want to stress that, here, we are estimating the wave impact by comparing two simulations. We thus believe that what matters the most is that all our simulations have been spun up for the same amount of time.

P5 L12: 'Updated floe size.' how is 'floe size' defined?
This is indeed unclear. The floe size in our study refers to the caliper diameter of the floes as defined by Rothrock and Thorndike (1984). We have added this information at the beginning of section 3 (P5L27).

P5 L14: 'floe size is actualized'. What does this mean? Also, P9 L11: What is 'actual floe size'? Similarly P9 L25: What is the 'actual FSD'?
We thank the reviewer for reporting these unclear expressions. The first one has been removed as the whole paragraph has been edited.
For the two other expressions mentioned, we simply removed the ambiguous word "actual", and we now refer to the FSD.

P5 L14: 'LIM3 takes into account the WRS in its ice transport equation'. This should be stated in the Introduction, as it is a key contribution of the manuscript.
We have added the following sentence in the last paragraph of the introduction:
P3L15 *"We focus in particular on two aspects of these interactions: firstly the effect of including the WRS, computed by the wave model, in the sea ice model, and secondly the wave-induced sea ice fragmentation and its effects on lateral melt through the addition of a FSD in the sea ice model."*

P6 L4: How is the partial sea ice cover already accounted for in WW3?
The estimation of sea ice-induced wave attenuation in WW3 is scaled by the sea ice concentration provided by forcing/coupling. As the WRS is directly proportional to this attenuation, it is therefore actually already scaled by the sea ice concentration. To make it clearer, we have rephrased our sentence as follows:
P6L20: "[...] *does not need to be multiplied by c, as the wave attenuation estimation in WW3 (and hence the WRS) is already scaled by the sea ice concentration to account for the partial sea ice cover."*

P6 L22: Define the sea ice thickness distribution and the FSD function. Is the latter an areal distribution?

In our model, the FSD is indeed an areal distribution (normalized by the cell area, just like sea ice fraction). Introduction to the sea ice thickness and floe size distribution has been added at the beginning of section 3.2. We have also added the following comment:
P8L6: *"From a technical point of view, the FSD in LIM3 is implemented as an areal distribution divided into floe size categories. It is advected in the same way as other sea ice tracers like sea ice concentration or thickness."*

P6 L22: I think a little more explanation would be useful here for readers not familiar with the various FSD schemes in the literature. Add a sentence or so on why the Zhang et al. (2015) approach is chosen over the Horvat et Tziperman (2015) approach. The sentence from P18 L13 'assuming floes of different sizes. . . ' should be stated here as well.
In their study, Horvat et Tziperman (2015) are using a thickness and floe size joint distribution in order to represent the evolution of sea ice floes affected by a great variety of processes, not necessarily related to waves (e.g. welding, refreezing, ridging...). Zhang et al. (2015) approach is simpler and computationally cheaper, as it assumes that all floes of a given size have the same ice thickness distribution, allowing the FSD to be treated independently from the sea ice thickness distribution. To do so, they hypothesize that the FSD mostly results from the fragmentation of large unbroken floes randomly yielding floes of any smaller size than the original ones.
Here, we choose to follow the simpler approach of Zhang et al. (2015), as we only consider the effects of wave-induced sea ice fragmentation and lateral melt on the FSD evolution, and our formulation of lateral melt does not depend on sea ice thickness (Steele, 1992). We have added these comments at the beginning of section 3.2 (P7L10), along with the definitions of floe size and sea ice thickness distributions.

P6 L28: 'implemented a FSD that enables floes to be advected..' – the FSD itself does not enable this, presumably this should say that Williams et al. (2017) implemented a scheme for advection of the FSD. Consider summarizing how this works e.g. what quantity is advected?
This part was actually misleading and has been rephrased. In reality, Williams et al. (2017) are using a Lagrangian model, in which they advect the maximum floe size by associating it with another quantity, the "number of floes", that is assumed to be conserved. This is not directly comparable to our case and we do not think it needs to be detailed.

P6 L31: 'We do not make any assumption on its shape in general, but the FSD is forced to follow the power-law assumed in WW3 as soon as wave-induced sea ice break-up occurs.' This sentence seems somewhat self-contradictory: there is an assumption on its shape if the FSD is constrained to follow a power-law.
The wording is indeed awkward. The paragraph describing the implementation of the FSD has been largely re-written, following other comments from the reviewer.

P7 L4: 'Assuming a power-law FSD is coherent with a distribution caused by a succession of break-up events (Toyota et al., 2011, Dumont et al. 2011).' The Toyota et al. 2011 study finds a change in the value of the exponent of a power-law fit to their data at around 40m. Does the model presented here assume a single power-law exponent, or include this transition?
Also note that the Toyota et al. 2011 study covers a small area in space and time, and therefore may not be globally applicable.

The Dumont et al. 2011 study itself does not show that a power-law FSD arises from a succession of break-up events, but rather provides a mathematical description for this assumption, so this citation should be removed or discussed in a different way.

As said before, the paragraph describing the implementation of the FSD has been largely re-written. More specifically, we answer the reviewer's questions:

- Here, we assume only a single power-law exponent, as done in the studies of Dumont et al. (2011) and Williams et al. (2013). As noted by Toyota et al. (2011), the value of the exponent of the FSD found for the large floe regime that they observe is too large (>2) to be solely due to repeated break-up of the sea ice floes. It is likely resulting from other processes, welding in particular. As we do not include such processes, we do not represent this transition.

- We have added a comment to highlight that Toyota et al. (2011) study covers a small area in space and time in the discussion section:
P18L32: "This assumption is made based on the observations analyzed by Toyota et al. (2011), that only sample a small area in time and space, so that their findings may not be applicable globally".

- We have removed the reference to Dumont et al. (2011) here.

P7 L8-22: The authors assume a power-law FSD in WW3 and then force LIM3 to follow the same power-law when wave fracture occurs. As they state, the effects of sea ice advection and thermodynamics cause deviations from a power-law. However, the effects of these processes may be over-ruled to continue to force the FSD to follow a power law, at a frequency determined by an arbitrary parameter. I don't understand why the authors take this approach. Why include other FSD processes if they are not always allowed to affect the FSD? How often does such over-ruling occur - is this most of the time or in a small fraction of timesteps? Is there an alternative approach to the power-law assumption? The assumption has not been well justified in the manuscript.
Similarly, can sea ice fracture be handled in the sea ice model rather than the wave model? I would have thought that this would avoid the need for the Dmax adjustment.
Again, the part describing the implementation of the FSD and the sea ice fragmentation has been largely re-written, as we agree that the choices we have made were not justified properly. We have also added a paragraph about the choices made regarding the FSD in the discussion section. Here we also try to explain our reasoning.

- The wording of our section, with the use of the terms "forcing" and "over-ruling" was indeed a bit awkward. The right word is actually "redistribution of the FSD", just like in Zhang et al. (2015). The difference is that instead of using a redistribution scheme that will lead to power-law FSDs with a varying exponent (as the scheme used by Zhang et al. does), our scheme redistributes the FSD to make it tend towards a power law with a constant exponent. This redistribution process has indeed a strong impact on the FSD, potentially erasing the effects of advection, but so it is in nature: fragmentation by waves is an instantaneous, violent phenomenon, that completely changes the FSD (see Collins et al. (2015) for the description of a fragmentation event).

- It is difficult to quantify the number of redistributions occurring in the model as it depends on the occurrence of fragmentation events, hence on local sea ice conditions and sea states. In general, fragmentation occurrences are higher when we get closer from the sea ice edge.

- Alternative approaches for the redistribution exist, like the one suggested by Horvat et Tziperman (2015). We added a comment on this topic in the discussion (P19L1).

- Handling the sea ice fragmentation in the sea ice model is indeed an option, however it would not solve the problem raised by the reviewer of defining the value of "Dmax" from the FSD. This variable is indeed needed by the wave model to estimate the wave attenuation. The problem of how to redistribute the sea ice after fragmentation would also remain.

P8 L3: 'This sensitivity remains really small.' This statement should be quantified more precisely, and the authors should describe how they determined this or consider adding their sensitivity results to Supplementary Material. Was sensitivity to the smallest resolved floe size tested? I would expect that lateral melt would be particularly sensitive to this.
We have performed several simulations with different numbers of categories (from 15 to 120) and different categories widths (from 2.5 to 20m) and did not find a strong sensitivity to those parameters. The results are however much more sensitive to the choice of Dmin (see our answer below).

P8 L16: Is this the same experiment as in Fig. 1? It would help the reader to re- state what the differences in the two runs correspond to physically. I think there are quite a few differences - evolving sea ice, advection of Dmax - which make it hard to understand what the differences in the model output mean.
These are indeed the same experiments as those presented in Fig. 1. We have added the following sentence to make it clearer:
P10L4: *In the uncoupled WW3 simulation, Dmax evolves depending on the sea state, but sea ice thickness and concentration are constant. In the WW3-LIM3 coupled simulation, sea ice properties are all evolving as sea ice is pushed by the WRS, and Dmax is advected with the FSD in LIM3.*

P9 L8: The Lupkes et al parametrization should be defined explicitly. Is this what LIM3 uses as standard for D in Eqn. 5? Please explain the reason for using it here.
The Lupkes parametrization is indeed what LIM3 uses as standard for D in Eqn. 5, and we therefore aimed to compare the standard parametrization to the one we included following Horvat et Tziperman (2015), which depends on the FSD. It has been clarified in the text:

P10L29: By *default, <D>, which represents the average floe size (referred to as the caliper diameter), is a function of the sea ice concentration obtained empirically from observational data by Lupkes et al. (2012).*

P9 L11: A situation where ice concentration is less than 0.6 and floe size is greater than 10 m could occur anywhere, for example near the ice edge in wave-free conditions, so I suggest removing the first part of this sentence.
We actually decided to remove the whole sentence as this effect is commented in section 4.

P9 L30: As stated above, I would expect the amount of lateral melt to depend strongly on Dmin. Have the authors investigated this? If not, the results on lateral melt should include some discussion of this.
This is a good point. To quantify this sensitivity, we ran again the simulations described in section 3.3 for 3 different values of Dmin: 4m, 8m (the standard value), and 16m. We find that

the dependency is particularly strong when using the formula of Lupkes et al.2012. After 4 days, the quantity of sea ice volume melted laterally is more than doubled when Dmin is reduced by a factor 2 (see figure below). Using the FSD to estimate the floe size significantly reduces this sensitivity, with a value of sea ice volume melted laterally after 4 days increasing by 26% between Dmin=8m and Dmin=4m, and decreasing by 18% between Dmin=8m and Dmin=16m.

The following figure and a new paragraph have been added in Section 3.3.

Section 4.1: This section compares the CPL and WAVE simulations at the pan-Arctic scale. The differences between the simulations include the impact of wave radiation stress and floe-size-dependent lateral melt. The authors then try to attribute various impacts to one of these two processes. Why not consider two separate runs here, one which adds the wave radiation stress only and one which adds the floe-size-dependent lateral melt only?
As it is, I found it difficult to understand this evaluation.
Section 4.1 in general was difficult to read. The text usually described differences to the CPL run. However, the WAVE and NO-CPL runs should be considered as the reference simulations, and so differences should be described in the CPL run relative to the reference runs (i.e. describe an increase in CPL relative to NO-CPL, rather than a decrease in NO-CPL). I think this would improve the readability.
We have largely edited this section to increase the readability, and to present the NO-CPL run as the reference (as this is already done in the figures). However, we do not think that we should include additional simulations and decompose even more the inclusion of the processes in the realistic set up. Indeed, we would have to compare too many runs and the text and figures would become too long and too numerous. We do believe that the current set of simulations allows us to describe and quantify the effect of each process.

P10 L19: It would help the reader to briefly restate the differences in the runs at the start of the paragraph, including the note at L27 ('One should keep in mind. . .). Also note mis-matched parentheses here.
We have added a short reminder of the differences between the simulations at the beginning of this paragraph (and thus removed the note at L27).

Sec. 4.1.3: The discussion of lateral melt would be aided by figures showing some equivalent floe size statistic from the Lupkes parametrization and from the FSD model.
This is not straightforward due to the different natures of the floe size in these two parameterizations. When using the Lupkes parameterization, the floe size is a scalar, that cannot be directly compared to a distribution as used in the coupled simulation. Comparing the scalar with the mean floe size from the FSD would not add value here.

P12 L11: 'This result does not reflect the fact. . .' What does this sentence mean?
We have rephrased this sentence:
P14L6*: "This result masks the fact…"*

P12 L17: 'Actually, in contrast to what was found in previous studies by Zhang et al. (2016), Bennetts et al. (2017), Roach et al. (2018a), de-activating completely lateral melt in both runs (not shown) has a negligible effect on the quantity of melted ice in our simulations (not shown).' The three named studies did not deactivate lateral melt, so the results presented here cannot be 'in contrast' to theirs. However, Roach, Dean, and

Renwick (2018) did essentially deactivate lateral melt, by setting all floe sizes to 10000m, and showed that this had no impact on sea ice concentration in the Antarctic.
The reviewer is right that our results cannot be directly compared to these previous papers. We have removed this sentence and replaced it by a statement highlighting that compensation of lateral melt enhancement by bottom melt decrease was also reported by Roach et al. (2018) and Bateson et al. (2019) (P14L12).

Section 4.2: This subsection is very interesting, but again hard to follow. Perhaps consider using one figure for each case, reducing the number of variables shown in figures in the main body of the paper, and moving the remainder to Supplementary Information. More figures could be added in the Supplementary for some of the 'not shown' aspects. I counted thirteen 'not shown' aspects in the paper, which seems rather high.
We have again edited this section, trying our best to streamline the text and increase its readability. In an earlier draft of this paper we have tried to make individual figures corresponding to the different cases, but it would require more figures than we have at the moment. Moreover, we do believe that the current organization of the figures helps the reader to comprehend the differences between the different cases.
In this section specifically, most of our 'not shown' occurrences refer to the conditions before the storms… while we do believe that it should be mentioned in the text because it helps explain the difference between the cases considered, we do not think that it would add much value to the paper to show these figures in Supplementary Material.

P16 L13: 'It is, however, mostly compensated by an increase of lateral melt.' Add that this is the converse of what has been shown in previous studies.
The text was actually 'compensated by an increase of bottom melt', which is similar to what was found by Bateson et al. (2019), as we now mention in the text.

P16 L8: 'The coupled model was then used to examine . . .. the effects of wave-induced sea ice break-up on sea ice melt.' Rather, the study compares their model to an alternative parametrization for lateral melt (the Lupkes parametrization), that is designed to approximate varying floe sizes for different concentrations. To isolate the impact of the wave-induced break-up, or the 'impact of the coupling' as mentioned earlier, a more suitable comparison would be to a simulation where all floes were unbroken. Otherwise, modify the discussion in the text.
We have changed the sentence to:
P18L6: "*(ii) the effects of using the wave-induced sea ice fragmentation to estimate lateral melt"*

P16 L30: Similarly, the paragraph at P16 L30 compares the difference in lateral melt between the FSD model and the Lupkes parametrization (with varying floe size) to the differences found in previous studies. However, these previous studies show differences between a FSD model and a constant floe size parametrization for lateral melt, so should not be directly compared to this study. The discussion of the various studies should reflect this.
We have modified the discussion to:
P19L22: *"Note also that we evaluate the impact of changing the lateral melt parameterization by comparing two simulations for which lateral melt depends on a varying floe size, either deduced from the FSD or estimated from the sea ice concentration using the parameterization suggested in Lüpkes et al. (2012). It differs from Zhang et al. (2016) who compare their FSD-model with a reference run without lateral melt, and from Roach et al. (2018) who use a constant floe size of*

300 m in their lateral melt parameterization. This might partly explain the discrepancies between our respective conclusions."

P17 L7: 'One should also remember that the studies of Zhang et al. (2016) and Roach et al. (2018b) were aiming at representing the evolution of floes larger than 1000 m.' This is incorrect. Both studies represent floes up to a maximum floe size of around 1000 m (radius). Also note that Roach et al. (2018a) and Roach et al. (2018b) are confused in places.

We agree that our sentence is not accurate, and we have rephrased it as follows:

P19L18: *"One should also remember that the studies of Zhang et al. (2016) and Roach et al. (2018) aimed to represent the evolution of floes with sizes ranging from a few cm to roughly 1 km on long time scales, whereas we focus on the important processes for wave-sea ice interactions and make the assumption that unbroken floes have a uniform floe size set to 1000 m."*

We have checked the occurrences of Roach et al. (2018a) and Roach et al. (2018b) carefully.

P17 L13: 'Among the wave-sea ice interaction processes. . .' This sentence is unclear. Impact on what?

We rephrased this sentence:

P19L28: "*Among the wave-sea ice interaction processes considered in this study, we find that the dynamical effect of the waves (the WRS) has a larger impact on sea ice conditions and sea surface properties than the modulation of lateral melt by sea ice fragmentation."*

Presentational Comments

Throughout, I would suggest referring to 'ocean surface waves' in the abstract and early parts of the Introduction, rather than simply 'waves' for clarity.
I would also suggest using 'sea ice fracture' rather than 'sea ice break-up,' as this is used in other studies

We have replaced 'wave' by 'ocean surface waves'. Regarding the use of 'sea ice break up', we have changed it to 'sea ice fragmentation' as we do believe that it is a more realistic representation of the process occurring. This terminology was already used in previous studies (e.g. Zhang et al. 2015).

In general, the definite article is over-used e.g. 'the sea ice near the sea ice edge' can simply be 'sea ice near the sea ice edge', 'impact the sea ice floe size' can be 'impact sea ice floe size' etc.

We accounted for these remarks and fixed the syntax mistakes: The paper has also undergone rephrasing in many parts with the help of native speakers in order to make it clearer.

P1 L3: 'In the present study....' - clumsy sentence, suggest rewording

Fixed

P1 'highlight the need to include the wave-sea ice processes in models aiming at fore-casting sea ice condition on short time scale' -> 'highlight the need to include wave-sea ice processes in models used to forecast sea ice conditions on short time scales'

Fixed

P2 L5: -> 'and sea ice drift'

Fixed

P2 L12: ‘in the direction of the propagation’

Fixed

P2 L13: ‘Southern ocean’ -> ‘Southern Ocean’

Fixed

P2 L14: ‘may become more prominent in the Arctic in the future.’

Fixed

P2 L27: ‘a first step was done’ -> ‘a first step was made’, similarly elsewhere progress is ‘made’ rather than ‘done’

Fixed

P3: reword ‘wave by sea ice’; ‘is implemented or not’; ‘without any wind or ocean current’; also the sentences on timestep

Fixed

P3 L14: change ‘on’ to ‘of’

Fixed

P4 L20: ‘aim at compensating’ -> ‘was made to compensate’

Fixed

P4 L31 ‘in this particular year’

Fixed

P4 L31: reword ‘storms occurring during it’

Fixed

P5 L1: ‘referred to as WAVE’

Fixed

P5 L9: sentences about average thickness - seem to use a lot of words to say some-thing fairly straightforward

Fixed

P5 L29: define vector k

Fixed

P7 L8: ‘the coupling between the two models can be done’ -> ‘the two models can be coupled’

Fixed

P10 L4: The introduction to Section 4 seems unnecessarily lengthy and should be made more concise.

Fixed

P10 L5: ‘the impact of the including the wave-sea ice interactions’ - reword

Fixed: The sentence has been changed to “*in order to quantify the impact of the coupling on wave, sea ice and ocean surface properties”*

P13 L25: ‘that is exposed upwind (and waves)’ - reword

Fixed (removing “and waves”)

P14 L19: ‘could in principle modified’ - reword

The whole sentence has actually been edited.

P14 L34 ‘very high waves of which attenuation induces WRS’ - reword

The sentence has been changed to *“the strong storm generates high waves, inducing a WRS as large as the wind stress close to the sea ice where most of the attenuation takes place.”*

P15 L14: ‘pattern than’ -> ‘pattern to’

Fixed

P15 L32 ‘low concentrated’ -> ‘of low concentration’

Fixed

P16 L15: ‘generating higher and more energetic waves’

Fixed

P17 L7: ‘were aiming at representing’ -> ‘aimed to represent’

Fixed

P17 L14: ‘additional lateral source melt’ - reword

Fixed

Section 4.1 figures – in the reference plots, I found the colormaps rather counter-intuitive. Consider choosing maps that are white at zero.

Fixed

Fig. 7: y-axis label lists the units as %, but values on the y-axis are out of 1. I presume that the 10ˆ2 kmˆ3 corresponds the numbers on the figure, but this should be noted in the legend.

Fixed

#Referee 3:

Anonymous Referee #3

The manuscript Toward a coupled model to investigate wave-sea ice interactions in the Arctic marginal ice zone by Boutin et al. presents a model that couples waves and sea ice dynamics to study the impact of waves on sea ice evolution over the Arctic Ocean. The model includes a floe size and thickness distribution as a prognostic variable that is exchanged between the sea ice and wave components. The FSTD obeys an evolution equation that includes floe-size dependent processes such as lateral melt and wave break-up. A focus is put on the wave radiation stress arising from wave attenuation in sea ice that imposes an additional force on the ice, and on the floe-size dependent lateral melt parameterization. The impact of wave-related processes on sea ice are studied by comparing simulations of NEMO-LIM3 (ice-ocean component) that is coupled and uncoupled to WW3 (wave component) over a pan-Arctic domain, and during two storm case. The comparison is done over a month-long period, at the end of summer 2010, after a 8-year spin-up period. Overall the paper makes a significant contribution to the modeling of polar marine environment in the sense that it provides a very useful tool to study the complexities wave-ice interactions and their impact over different spatio-temporal scales. The discussion puts the study in the context of the recent developments and describes the limitations, thus pointing towards important issues to be addressed in order to make further progress (duration of the simulation, atmospheric and oceanic coupling, floe-size dependent ice rheology missing, freezing period not studied, etc.). It is well written, despite some typos and corrections that need to be made, and descriptions of model implementation and results are detailed enough, although some key information is missing (see below). It is thus worthy of publication, after minor revisions are made.

We thank the reviewer for their careful reading of our manuscript and for their comments and suggestions. We have tried to address their questions and concerns, as detailed in the following. In our comments, PXLY refers to page X line Y of the attached updated manuscript.

Specific comments

P4. L18. Wave attenuation is a central piece of the study, as it determines the wave radiation stress and, to a certain extent, the extent of the wave-induced ice break-up area (i.e. the marginal ice zone). Because of this, I suggest that in addition to referring to Ardhuin et al. (2018) for the choice of the wave attenuation, authors recall the main characteristics of the attenuation scheme. Is it floe-size and/or thickness dependent,and how? Is it a dissipative or scattering scheme (or a mix of both)? This could be done in a few lines.

We have added a short description of the processes described in Ardhuin et al. (2018) and Boutin et al. (2018) in P3L27.

P6. L1. Another central piece of the study is the ice drift resulting from the momentum balance. Here the WRS is added as an external forcing term that will be balanced by the internal stress, and model solutions may depend strongly on rheology

parameters. I understand that this term (rheology) has not been modified significantly from what's typically used by LIM3 users, and that studying the ie rheology is not the focus of the paper, but it needs to be described minimally here. The rheology contains a few parameters that can be tuned for various reasons, including the compressive strength, the shear-to-compressive strength ratio, if not the yield curve itself or the numerical scheme. Describe what rheology is used and what are the main parameter values. Maybe adding a table would serve well that purpose.

We have added a few comments along with details on the parameters used in the rheology in section 2:
P3L32*: "The model includes a standard Elasto-Visco-Plastic rheology (Hunke and Dukowicz, 1997), using the stress tensor formulation of Bouillon et al. (2013) adapted for the C-grid used in the model. The ice strength is determined following Hibler III (1979), with the ice strength P following* $P = P^* h e^{C(1-c)}$*, where P*=20,000 N/m2 and C=20 are empirical positive parameters, and h is the cell-average sea ice thickness. The plastic failure threshold lies on an elliptical yield curve of which eccentricity is set equal to 2. The number of sub-time steps used to solve the momentum equation is set to 120."*

P11. L14. Warmer and saltier surface waters in the CPL run seems to point towards that enhanced turbulent mixing arising by increased shear stress between the ice and the ocean, dominates over enhanced melting, which tends to produce fresh and cold anomalies. The following section focuses on an interpretation of that response in terms of the differences between the lateral melt parameterization. Have you looked at mixing as a possible mechanism for explaining it? Are there anomalies in the mixing or mixed layer depth in the marginal ice zone? This mechanism is discussed very clearly later in the two storm cases, but it would be interesting to discuss it also for the pan-Arctic case.
We had a look at the differences in mixed layer depth and properties, but the signal was very patchy, making it difficult to draw conclusions at the pan-Arctic scale. Indeed, we do believe that local conditions matter a lot (e.g., the relative directions of the wind, sea ice, waves, and surface currents) in determining the impact of the waves, which motivated us to investigate regional cases.

P19. Eq A3. Define D_*. And later, define also n_*. Is D_* equivalent to D_{n*}?

Explicit definitions of these terms have been added in the appendix (P21L18,P22L6).

Some typos

P5. L14. Replace actualized by updated.
Fixed
P5. L20....is transferred to what has caused this attenuation.
Fixed
P5. Eq2. Remove parentheses aroundσ.
Fixed

P6. L22. multi-category.
Fixed
P7. L29.c has already been introduced as the concentration earlier.
We think a reminder might help the reader there.
P8. L10. Is Toyota et al. (2011) the right reference for this statement? There are older and more appropriate references for this it seems. The smallest floe size that can be generated by flexural break-up is thickness-dependent. Maybe this should be acknowledged.
We now cite Mellor (1986) instead. This study suggests a formulation for this lower limit of floe size that can break due to flexural break-up.The fact that this lower limit is thickness dependent is true but adding it to the text might add confusion in our opinion, as this paragraph focuses on the definition of floe size categories with constant upper and lower limits.

P8. L25. Uncoupled instead of not coupled (also at various other place in the manuscript).
Fixed
P9. L8. Based on a number of observations.
Fixed
P9. L17. Rather than on sea ice conditions.
Fixed (with concentration instead of conditions)
P10. L8....on sea ice conditions.
Fixed
P10. L19. There is no panel e on Fig. 5.
Fixed
P11. L9. Do you refer to the grid cell average thickness?
Yes, we edited so that it is now clearly specified.
P11. L11. There are also differences…
Fixed
P12. L1....property anomalies.
Fixed (we kept the word *difference* to keep coherency with the rest of the text)
P14. L6. Difference (singular).
Fixed
P17. L24. when trying to forecast…
Fixed
Fig2. Schematic summary of...The two boxes correspond…
Fixed
Fig3. Panel c. notcpl should be replaced by NOT_CPL in the index. You can also specify the run elsewhere than in the index to avoid expanding indices.
Fixed
Fig5. The black and grey contours…
Fixed

~~Toward~~ Towards a coupled model to investigate wave-sea ice interactions in the Arctic marginal ice zone

Guillaume Boutin[1], Camille Lique[1], Fabrice Ardhuin[1], Clément Rousset[2], Claude Talandier[1], Mickael Accensi[1], and Fanny Girard-Ardhuin[1]

[1]Univ. Brest, CNRS, IRD, Ifremer, Laboratoire d'Océanographie Physique et Spatiale, IUEM, Brest, France
[2]Sorbonne Universités (UPMC Paris 6), LOCEAN-IPSL, CNRS/IRD/MNHN, Paris, France

Correspondence: boutinguillaume87@gmail.com

Abstract. The Arctic Marginal Ice Zone (MIZ), where strong interactions between sea ice, ocean and atmosphere are taking place, is expanding as the result of ~~the~~ on-going sea ice retreat. Yet, ~~state-of-art models are not capturing the complexity of the varied processes occurring in the MIZ, and in particular the processes involved in the~~ state-of-the-art models exhibit significant biases in their representation of the complex ocean-sea ice interactions ~~. In the present study, a coupled sea ice - wave model is developed, in order to improve our understanding and model representation of those interactions. The coupling allows us~~ taking place in the MIZ. Here, we present the development of a new coupled sea ice-ocean wave model. This set up allows us to investigate some of the key processes at play in the MIZ. In particular, our coupling enables to account for the wave radiative stress resulting from the wave attenuation by sea ice, and the sea ice lateral melt resulting from the wave-induced sea ice ~~break-up. We found~~ fragmentation. We find that, locally in the MIZ, the ocean surface waves can affect the sea ice drift and melt, resulting in significant changes in sea ice concentration and thickness as well as sea surface temperature and salinity. Our results highlight the need to include ~~the~~ wave-sea ice processes in models ~~aiming at forecasting~~ used to forecast sea ice conditions on short time ~~scale, although~~ scales. Our results also suggest that the coupling between waves and sea ice would ~~probably required~~ ultimately need to be investigated in a more complex system, allowing for interactions with the ocean and the atmosphere.

1 Introduction

Numerical models exhibit large biases in their representation of ~~the~~ Arctic sea ice concentration and thickness, regardless of their complexity or resolution (Stroeve et al., 2014; Chevallier et al., 2017; Wang et al., 2016; Lique et al., 2016). Comparing 10 reanalyses based on state-of-the-art ocean-sea ice models against observations, Uotila et al. (2018) found that ~~the model biases are~~ model biases were the largest in the Marginal Ice Zone (MIZ). Indeed, the MIZ is characterized by a wide variety of processes resulting from the highly ~~non-linear~~ non-linear interactions between the atmosphere, ~~the ocean and the sea ice(Lee et al., 2012),~~ ocean and sea ice: sea ice floe fragmentation and welding, lead opening and associated heat transfers, mesoscale and submesoscale features arising from strong temperature and salinity gradients (see Lee et al., 2012, for a review and reference , and many of these processes are only crudely (if at all) taken into account in models. Some of these processes~~result from the~~

~~interactions between surface wave~~ , sea ice fragmentation in particular, result from interactions between ocean surface waves and sea ice, and are thought to be key for the dynamics and evolution of the MIZ (Thomson et al., 2018). These interactions are the focus of the current paper.

~~Summer sea~~

Sea ice in the Arctic has been drastically receding over the past few decades (Comiso et al., 2017), resulting in an expansion of the MIZ in summer (Strong and Rigor, 2013) which is expected to ~~be intensified~~ intensify in the future (Aksenov et al., 2017). This ~~offers~~ provides an expanding fetch for waves to grow and propagate ~~(Thomson and Rogers, 2014)~~ (Thomson and Rogers, 2014; Waseda et al., 2018), suggesting an overall increase of wave heights in the Arctic ~~(Stopa et al., 2016b)~~ (Stopa et al., 2016a). Once generated, waves can then propagate into sea ice, ~~impacting strongly the dynamical and thermodynamic~~ strongly impacting both dynamical and thermodynamical sea ice properties in the MIZ through different mechanisms (Asplin et al., 2012). First, observations suggest that waves determine the shape and size of the sea ice floes in the MIZ, through the ~~break-up~~ fragmentation occurring when the ice cover is deformed (Langhorne et al., 1998), or by controlling the formation of frazil/pancake ice (Shen and Ackley, 1991). Wave-induced sea ice fragmentation is also expected to affect lateral melt (Steele et al., 1992), heat fluxes between ocean and atmosphere (Marcq and Weiss, 2012), ~~or~~ and sea ice drift in the MIZ (McPhee, 1980; Feltham, 2005; Williams et al., 2017). When breaking in the MIZ, waves can generate turbulence in the mixed layer (Sutherland and Melville, 2013), possibly affecting the rate of ice formation or melting by modulating heat fluxes between the ocean, the sea ice and the atmosphere. Observations conducted during a storm in October 2015 in the Beaufort Sea have~~for instance~~ , for instance, revealed that storm-induced waves can lead to an increase of surface mixing and an associated heat entrainment from the upper ocean, resulting in ~~an important~~ large melt of pancake ice (Smith et al., 2018). Finally, waves transport momentum, ~~so that~~ and therefore when they are attenuated in the MIZ through reflection or dissipation, part of ~~the~~ their momentum goes into sea ice. This process, called ~~the~~ wave radiative stress (WRS; Longuet-Higgins and Stewart, 1962; Longuet-Higgins, 1977), acts as a force that pushes the sea ice in the direction of ~~the~~ propagation of the attenuated waves. This force is a dominant term in the ice momentum balance ~~on the outskirts of the Southern ocean sea ice~~ in the Southern Ocean MIZ (Stopa et al., 2018b) and it may become more prominent in the Arctic in the future. In return, sea ice strongly attenuates waves propagating in the MIZ, either by dissipative processes (e.g. under-ice friction, inelastic flexure, floe-floe collisions) or conservative processes (e.g. scattering) (Squire, 2018).

Most of the recent efforts in the ~~modeling~~ modelling community have been ~~focusing~~ focused on the impact of sea ice on waves (Dumont et al., 2011; Williams et al., 2013; Montiel et al., 2016), leading to the development of wave models accounting for the presence of sea ice ~~(Dumont et al., 2011; Williams et al., 2013; Montiel et al., 2016; Boutin et al., 2018)~~(Boutin et al., 2018) . By prescribing sea ice conditions, these models are able to ~~reproduce accurately~~ accurately reproduce the time and space variations of wave ~~height~~ heights in sea ice retrieved from recent field observations (Kohout et al., 2014; Thomson et al., 2018; Cheng et al., 2017) and innovative processing of Synthetic Aperture Radar (SAR) satellite observations (Ardhuin et al., 2017). The good agreement with the observations also suggests a proper representation and quantification of ~~the~~ wave attenuation and propagation in sea ice in these models (Ardhuin et al., 2016; Rogers et al., 2016; Ardhuin et al., 2018). Yet, in this case, sea ice

conditions are only a forcing and thus not affected by waves. This means that these models cannot realistically represent the fate of the sea ice floes once broken by waves, as they do not account for advection, melting and refreezing processes. A first step ~~toward~~ towards the representation of ~~the~~ wave-sea ice interactions was ~~done~~ made by Williams et al. (2013) and Boutin et al. (2018), who included in their respective ~~model~~ models a Floe Size Distribution (~~hereafter~~ FSD) that evolves depending on the sea state. ~~Yet~~However, considering only ~~the~~ sea ice fragmentation is not sufficient to represent the full complexity of ~~the~~ wave-sea ice interactions.

In ~~contrast, little progress has been done~~ parallel, progress has also been made regarding the inclusion of the effects of waves in coupled ocean-sea ice models. Using a very simple parameterization, Steele et al. (1989) and Perrie and Hu (1997) have investigated the effect of WRS on ~~the~~ sea ice drift in the MIZ, only considering the attenuation of waves generated between the ice floes~~. They~~ , and found a limited impact on the sea ice conditions. More recently, Williams et al. (2017) ~~have~~ implemented a wave module in the ~~semi-lagrangian~~ semi-Lagrangian sea ice model neXtSIM (Rampal et al., 2016) and found that high ~~waves conditions can induce~~ wave conditions can cause a significant displacement of the sea ice edge. The implementation of FSDs in different sea ice models~~as done by Zhang et al. (2015) or Horvat and Tziperman (2015) has also allowed the~~ , as introduced by Zhang et al. (2015) and Horvat and Tziperman (2015) for instance, has also opened the way to the assessment of the potential enhancement of lateral melt by wave-induced ice fragmentation ~~(Zhang et al., 2016; Bennetts et al., 2017)~~ (Zhang et al., 2016; Bennetts et al., 2017; Roach et al., 2018; Bateson et al., 2019), but the representation of waves remains too ~~crude~~ simple to simulate the full effect of waves on the evolution of sea ice.

In the present study, we go beyond ~~the simple inclusion of the forcing of wave~~ simply forcing a wave model by sea ice ~~or of sea ice by wave in models~~properties, or conversely forcing a sea ice model by wave properties, by proposing a full coupling between a spectral wave model and a ~~state-of-art~~ state-of-the-art sea ice model. The coupled framework allows us to investigate the interactions between waves and sea ice in the Arctic, and the impact that including these effects in a model has on the representation of the ~~wave~~waves, ocean, and sea ice properties in the Arctic MIZ. We focus in particular on two aspects of these interactions: firstly the effect of including the WRS, computed by the wave model, in the sea ice model, and secondly the wave-induced sea ice fragmentation and its effects on lateral melt through the addition of a FSD in the sea ice model. The remainder of this paper is organized as follows. The different models and configurations used in this study are described in Section 2. Section 3 is devoted to the theoretical and practical implementation of the coupling between the two models. In section 4, we compare ~~pan-Arctic simulationsin~~ two pan-Arctic simulations: one for which the coupling between wave and sea ice is implemented~~or not, in order~~ , and one with the ocean-sea ice model run as stand-alone. Our objective is to quantify the dynamical and thermodynamical impacts ~~on~~ of the coupling on the sea ice and ocean surface properties. A summary and conclusions are given in Section 5.

2 Methods

In this study we make use of the spectral wave model WAVEWATCH III® (hereafter WW3; The WAVEWATCH III ® Development Group, 2016), building on the previous developments ~~performed~~ by Boutin et al. (2018) who included a FSD in WW3 as well as a representation of the different processes by which sea ice can affect the propagation and ~~modulation~~ attenuation of waves in the MIZ. These processes are scattering (which redistributes the wave energy without dissipation), friction under sea ice (with a viscous and a turbulent part depending on the wave Reynolds number), and inelastic flexion. All these processes depend on sea ice thickness and concentration, and scattering and inelastic flexion also depend on floe size.

We also use the sea ice model LIM3 (Vancoppenolle et al., 2009; Rousset et al., 2015), in which a FSD is first implemented as described in Section 3.2. The model includes a standard Elasto-Visco-Plastic rheology (Hunke and Dukowicz, 1997), using the stress tensor formulation of Bouillon et al. (2013) adapted for the C-grid used in the model. The ice strength is determined following Hibler III (1979), with the ice strength P following $P = P^* h e^{C(1-c)}$, where P^*=20,000 N/m^2 and C=20 are empirical positive parameters, and h is the cell-average sea ice thickness. The plastic failure threshold lies on an elliptical yield curve, with the eccentricity set to 2. The number of sub-time steps used to solve the momentum equation is set to 120. The two models are coupled through the coupler OASIS-MCT (Craig et al., 2017). Two configurations of different complexities are used in the following and briefly described in the ~~remaining~~ remainder of this section.

2.1 Idealized configuration

In order to test and illustrate the effect of the coupling (Section 3), we make use of a simple idealized configuration (see Fig. 1), in which LIM3 is used in a ~~stand alone~~ stand-alone mode (without any ocean component). The configuration is a squared domain with 100×100 grid ~~cell~~cells, with a resolution of 0.03^o in both directions (corresponding roughly to 3 km). Both models are run on the same grid ~~, and~~ with the same time step set to 300s. The coupling time step is also set to 300s~~too~~. The sea ice is ~~only forced~~ forced solely by waves, without prescribing any wind or ocean ~~current~~currents. Following Boutin et al. (2018), the simulation starts at rest, with distributions of sea ice concentration (Fig. 1a) and thickness (Fig. 1c) set to represent roughly the conditions that can be found in the MIZ. Starting from the western border, the domain is free of ice over the first $\simeq$10 km, after which the ice concentration c increases linearly from 0.4 to 1 about 90 km further eastward (longitude=0.84^{o}E). Ice thickness also increases from west to east following $h_i = 2(0.1 + \mathrm{e}^{-N_x/20})$, where N_x is the number of grid cells in the ~~x direction~~ x-direction starting from the western border of the ~~ice covered~~ ice-covered domain. Waves radiate from part of the western border of the domain, between 1.2 and 1.8^o ~~of~~ latitude, and propagate to the east. The wave spectrum used as forcing at the boundary is extracted at a point south of Svalbard from an Arctic ~~realistic simulation using~~ hindcast performed with WW3 described by Stopa et al. (2016a)~~for~~. It covers the period of May 2nd ~~and~~ to 3rd, 2010, during which a storm ~~happened south of Svalbard~~ occurred in this particular area (Collins et al., 2015). Here we rotate the spectrum so that the direction with the largest density of wave energy is lined up with our x-axis. Simulations start on April 30th, at 02:00 a.m., and the attenuation processes (scattering, bottom friction and inelastic flexion dissipation) use the same parameterization as in the reference simu-

lation described by Ardhuin et al. (2018).

2.2 Pan-Arctic configuration

We also make use of the CREG025 configuration (Dupont et al., 2015; Lemieux et al., 2018), which is a regional extraction of the global ORCA025 configuration developed by the Drakkar consortium (Barnier et al., 2006). Although the coupling is solely between ~~the~~ LIM3 and WW3, the configuration here also includes the ocean component of NEMO 3.6 (Madec, 2008). CREG025 encompasses the Arctic and parts of the North Atlantic down to ~~27~~26^o, and has 75 vertical levels and a nominal horizontal resolution of 1/4^o($\simeq$ 12 km in the Arctic~~basin~~). Both NEMO-LIM3 and WW3 are run on the same grid. Initial conditions for the ocean are taken from the World Ocean Atlas 2009 climatology for temperature and salinity. The initial sea ice thickness and concentration are taken from a long ORCA025 simulation performed by the Drakkar Group. Along the lateral open boundaries, monthly climatological conditions (comprising sea surface height, 3-D velocities, temperature and salinity) are taken from the same ORCA025 simulation. Regarding the atmospheric forcing, we use the latest version of the Drakkar Forcing Set (DFS 5.2, which is an updated version of the forcing set described in Brodeau et al., 2010). The choices regarding the parameterization of the wave-ice attenuation are following the ones made in the *REF* simulation by Ardhuin et al. (2018). The ~~value of the~~ ice flexural strength has however been increased from 0.27 MPa to 0.6 MPa, which is the highest value used in Ardhuin et al. (2018). This choice makes sea ice harder to break, and ~~aim at compensating~~ has been made to compensate the fact that no lateral growth of sea ice is included in our coupled framework.

Three simulations are performed. First we run a simulation based solely on NEMO-LIM3 (referred to as NOT_CPL), covering the period from January 1st, 2002 to the end of 2010, in which the already existing lateral melt parameterization ~~from Lüpkes et al. (2012)~~ in LIM3 is activated. The first years of the simulations are allowing for the adjustment of the ocean and sea ice conditions and we only analyze results from August and September 2010. During that period, the sea ice extent reaches its annual minimum, providing some fetch for the generation of ~~sea ice, and~~ waves, in particular in the Beaufort Sea. The model sea ice extent during the summer of 2010, and more generally the distribution of the sea ice concentration, compares reasonably well with satellite observations (not shown). Note that this period includes a drop in sea ice concentration in the ~~Central~~ central Arctic, found both in model results and in satellite observations, that has already been documented by Zhao et al. (2018) and attributed to an enhancement of ice divergence in this region in this particular year. This specific period has also been ~~chosen as some storms occurred during it , so that extreme waves~~ selected as it includes a few storm events, so extreme wave conditions can be investigated. Another simulation (CPL) is initialized from NOT_CPL on August 1st 2010 and run until September 9th 2010. After ~~that~~ this date, sea ice extent starts to increase again, and as our FSD distribution does not allow for the refreezing of ~~the~~ sea ice floes, we cannot ~~represent realistically~~ realistically represent the processes at play during ~~that~~ this period.

Finally, we run a simulation over the same period, based solely on WW3 (referred to as WAVE), in which the wave model is forced by sea ice conditions from the NOT_CPL simulation. In order to allow for some spin up for the waves to develop and

break the ice, we remove the first 3 days. In the following, all the results are for the ~~37-days~~ 37-day period between August 4th and September 9th 2010.

3 Implementation of the coupling between the wave and ~~the~~ sea ice models.

The objective of this section is to present the theoretical background and the practical implementation of the coupling between LIM3 and WW3. Fig. 2 shows the principle of the coupling and the variables that are exchanged between the two models. Briefly, LIM3 provides sea ice floe size, thickness and concentration to WW3 in order to estimate the wave attenuation and wave-induced sea ice ~~break-up~~fragmentation. Note that ~~LIM3 being a multi-category sea ice model, the actual state variable is a~~ in our study, the floe size refers to the caliper diameter of the floes as defined by Rothrock and Thorndike (1984). We refer to sea ice thickness ~~distribution g_h, from which the mean~~ as the cell-average of the sea ice thickness ~~can be defined either by doing a grid-cell average or by doing an ice-cover average. Here we choose to~~ distribution g_h used as a state variable in LIM3. In the coupling, we actually exchange the ice-cover average sea ice thickness, although this choice does not ~~affect significantly~~ significantly affect our results. WW3 then returns the WRS to LIM3, as well as the updated floe size if fragmentation has occurred. LIM3 takes into account the WRS in its ice transport equation, and advects the sea ice and its information on floe size. ~~If break-up~~ This information is carried by a newly implemented FSD, the sea ice concentration being distributed among floe size categories. If fragmentation has occurred in the wave model, ~~floe size is actualized to match the FSD~~ the FSD in LIM3 is re-arranged, transferring sea ice from large floe categories to smaller floe categories. The resulting FSD obeys a power-law similar to the one assumed in WW3. The ~~floe size~~ FSD is then used to estimate lateral melt.

In the following, we describe in more ~~details~~ detail the modifications that have been ~~done~~ carried out in LIM3 and WW3 in order to couple them, and how variables are exchanged between the two models. The coupling allows a new formulation for the sea ice lateral melt in LIM3 (section 3.3).

3.1 Wave Radiative Stress

Waves transport momentum, and when they are attenuated either by dissipation or ~~reflections~~reflection, this momentum is transferred to ~~the cause of~~ what has caused this attenuation (Longuet-Higgins, 1977). In the case of sea ice, this momentum loss thus acts as a stress that pushes sea ice in the direction of attenuated waves. Following the study of Williams et al. (2017), in which a WRS was implemented in neXtSIM, the WRS $\tau_{w,i}$ is computed as:

$$\tau_{w,i} = \rho_w g \int_0^{\infty} \int_0^{2\pi} \frac{-S_{\text{ice}}(\mathbf{x};\omega,\theta)}{\omega/k} (\cos\theta, \sin\theta) d\theta d\omega \tag{1}$$

where ρ_w is the water density, g is gravity, ω, θ and k are respectively the radial frequency, direction and wavenumber of waves and $S_{\text{ice}}(\mathbf{x};\omega,\theta)$ is the source term (negative by convention in WW3) corresponding to wave attenuation by sea ice at a given position.

Once estimated by WW3, the WRS is then sent to the sea ice model and added as an additional term in the momentum equation of LIM3 (Rousset et al., 2015):

$$mD_t\mathbf{u} = \nabla \cdot (\boldsymbol{\sigma}) + c(\tau_a + \tau_o) + \tau_{w,i} - mf\,\mathbf{k} \times \mathbf{u} - mg\nabla\eta, \quad (2)$$

in which m is the total mass of ice and snow per unit of area, $\mathbf{u}$ is the ice velocity vector, $\boldsymbol{\sigma}$ is the internal stress tensor, f is the Coriolis parameter, k is a unit vector pointing upwards, η is the sea surface elevation, c is the sea ice concentration, and τ_a, τ_o are the atmospheric and oceanic stresses, respectively. In contrast to τ_a and τ_o, $\tau_{w,i}$ ~~doesn't require~~ does not need to be multiplied by c, ~~since the~~ as the wave attenuation estimation in WW3 (and hence the WRS) is already scaled by the sea ice concentration to account for the partial sea ice cover~~is already accounted for in WW3~~.

Fig. 1 illustrates the effect of the implementation of the WRS in our simple model. Here, the sea ice thermodynamics ~~is~~ are switched off, so that we only ~~simulated~~ simulate the effect of waves pushing sea ice. Under the action of waves, the sea ice edge shifts eastward, resulting in an increase of the sea ice concentration (panel b). As the sea ice near the sea ice edge is compacted, it creates a sharp gradient in sea ice concentration and thickness (panels b,~~e~~d). When comparing panels (e) and (f), it is clear that wave attenuation also responds to this change of the sea ice properties: waves tend to penetrate further eastward when the sea ice edge retreats to the east, but are then attenuated faster in the compacted sea ice.

3.2 Floe size distribution and sea ice ~~break-up~~fragmentation

As mentioned earlier, waves can break sea ice and thus impact the sea ice floe size. It is ~~thus required to exchange a FSD~~ therefore necessary to exchange information on floe size between the two models, which can be done by using a FSD. A FSD has been previously implemented in WW3 by Boutin et al. (2018), and is used to estimate the wave attenuation due to inelastic flexure and scattering. Following the work by Toyota et al. (2011) and Dumont et al. (2011), we assume that the FSD in WW3 follows a truncated power law between a minimum floe size, $D_{\min}$ and a maximum floe size, $D_{\max}$. $D_{\min}$ corresponds to the minimum floe size that can be generated by waves and is of the order of $O(10\text{m})$, while $D_{\max}$ depends on the local ~~waves~~ wave properties and is used to estimate the level of sea ice fragmentation.

There is no FSD included in the standard version of LIM3. However, recent work by Zhang et al. (2015) and Horvat and Tziperman (2015) ~~have~~ has proposed ways to implement a FSD in sea ice models, following what is done for the sea ice thickness distribution (which is a state variable of any ~~multi category~~ multi-category sea ice model). ~~Here we start by following the~~ In their study, Horvat and Tziperman (2015) use a joint thickness and floe size distribution in order to represent the evolution of sea ice floes affected by a great variety of processes not necessarily related to waves (i.e welding, refreezing, ridging...). The approach by Zhang et al. (2015) is simpler and computationally cheaper, as it assumes that all floes of a given size have the same ice thickness distribution, allowing the FSD to be treated independently from the sea ice thickness distribution. To do so, they hypothesize that the FSD mostly results from the fragmentation of large unbroken floes randomly yielding floes of any size smaller than the original ones. In this study, we choose to follow the simpler approach of Zhang et al. (2015), ~~distributing ice~~

~~concentration into bins corresponding to different floe sizes by defining a FSD function g_D.~~ as we only consider the effects of wave-induced sea ice fragmentation and lateral melt on the FSD evolution, and our formulation of lateral melt does not depend on sea ice thickness (see section 3.3). Therefore, we can consider the distribution of sea ice thickness and floes independently, defined respectively as:

$$\int_{h}^{h+dh} g_h(h)dh = \frac{1}{A}a_h(h, h+dh) \tag{3}$$

$$\int_{D}^{D+dD} g_D(D)dD = \frac{1}{A}a_D(D, D+dD) \tag{4}$$

and respecting:

$$\int_{0}^{\infty} g_h(h)dh = 1 \tag{5}$$

$$\int_{0}^{\infty} g_D(D)dD = 1, \tag{6}$$

h being the sea ice thickness and D still being the caliper diameter of the floes as defined by Rothrock and Thorndike (1984). In these definitions, A is the total area considered, and a_h and a_D are the areas within A covered by sea ice with thickness between h and $h+dh$ and floes with diameters between D and $D+dD$ respectively. The evolution of the FSD depends on sea ice advection, thermodynamics and mechanical processes, and is given by:

$$\frac{\partial g_D}{\partial t} = -\nabla \cdot (\mathbf{u} g_D) + \Phi_{th} + \Phi_m, \tag{7}$$

in which $\mathbf{u}$ corresponds to the sea ice velocity vector, Φ_{th} is a redistribution function of floe size due to thermodynamic processes (*i.e* lateral growth/melt), and Φ_m is a mechanical redistribution function associated with processes like fragmentation, lead opening, ridging, and rafting. From a technical point of view, the FSD in LIM3 is implemented as an areal distribution divided into floe size categories. It is advected in the same way as other sea ice tracers like sea ice concentration or thickness.

In their sea ice model neXtSIM, Williams et al. (2017) have also implemented a FSD ~~that enables the floes to be advected once they have been broken by waves, making the assumption~~ but in a different way than Zhang et al. (2015). Indeed, they assume that the FSD follows a truncated power-law between a minimum and ~~a~~ maximum floe size, ~~similarly~~ similar to the assumption made in WW3. ~~Here we take a similar approach and~~ Thus, in their model, the FSD always obeys a power-law with a constant exponent, and only evolves when sea ice fragmentation results in a reduction of the maximum floe size. Here we combine the approaches of Zhang et al. (2015) and Williams et al. (2017) and implement a FSD in LIM3 that evolves following ~~eq.(7). Yet~~Eq.7, but that also undergoes a redistribution after each fragmentation event that makes it tend towards the

power-law assumed in WW3. Thus, in contrast to Williams et al. (2017), we do not make any assumption ~~on its shape~~ about the shape of the FSD in general, but~~the FSD is forced to follow the~~ , just as they do, we assume that after being fragmented by waves, the FSD follows a power-law ~~assumed in WW3~~ with a maximum floe size that depends on the local sea state. Our implementation only differs from the one done by Zhang et al. (2015) in the way we have implemented the redistribution: instead of assuming that the broken sea ice is redistributed uniformly among the smaller floes after each fragmentation event (that actually quickly tends towards a power-law distribution with a varying exponent depending on the wave state in their study), our redistribution is set to a power-law with a constant exponent as soon as ~~wave-induced sea ice break-up occurs. This ensure coherence between the FSDs in LIM3 and WW3. We acknowledge that this assumption on the FSD is strong, and as discussed in Roach et al. (2018), it is not a suitable way to proceed when studying the sea ice evolution, since the FSD should evolve freely and observation have regularly shown that power-law distributions are not always followed (e.g. Inoue et al., 2004). However, understanding the details of~~ fragmentation occurs. We justify this choice of redistribution scheme by the fact that fragmentation is a violent process, that can completely change a FSD in time scales of a few minutes to a few hours (see Collins et al., 2015, for the description of such an event). Note that the redistribution of the FSD due to fragmentation transfers sea ice from large floes to smaller floes. Combined with lateral melt, a process that also reduces the floe size, the ~~FSD evolution is beyond the scope of this study, and assuming a power-law FSD is coherent with a distribution caused by a succession of break-up event (Toyota et al., 2011; Dumont et al., 2011)~~action of waves in our model always reduces the floe size. The details of the mechanical redistribution function Φ_m are mostly following what has been proposed by Zhang et al. (2015) and are given in appendix A.

Now that both models include a FSD, the ~~coupling between the~~ two models can be ~~done~~ coupled in order to represent the effect of the wave-induced sea ice ~~break-up, whose occurrence~~ fragmentation, the occurrence of which in LIM3 is determined depending on information provided by WW3. As mentioned earlier, sea ice ~~break-up~~ fragmentation in WW3 is controlled by local wave properties~~and break-up~~ , and fragmentation events result in an update of the maximum floe size $D_{\max}$. It is thus logical to define a similar parameter $D_{\max,\mathrm{LIM3}}$ from the ~~LIM3's FSD , that would~~ FSD of LIM3, that ideally equals $D_{\max}$. ~~Yet~~ However, estimating $D_{\max,\mathrm{LIM3}}$ is not straightforward. Indeed, our FSD implementation requires that $D_{\max,\mathrm{LIM3}}$ corresponds to the upper limit of the power law followed by the FSD in both WW3 and LIM3, but also that $D_{\max,\mathrm{LIM3}}$ can evolve with the deviations of the FSD in LIM3 ~~'s FSD~~ from this power-law under the effects of sea ice advection and thermodynamics. Calling $g_{D,\mathrm{P.L}}$ the distribution corresponding to a FSD following the assumed power-law, we thus define $D_{\max,\mathrm{LIM3}}$ as the greatest value of D for which the following condition applies:

$$\int_D^\infty g_D dD \geq k_{D_{\max}} g_{D,\mathrm{P.L}}, \tag{8}$$

in which $k_{D_{\max}}$ is an *ad hoc* parameter allowing the value of $D_{\max,\mathrm{LIM3}}$ to remain unchanged when the FSD slightly deviates away from the assumed power-law (after lateral melt or advection for instance). Setting $k_{D_{\max}}$=1 is ~~a too strong~~ too strong a constraint, and results in noisy $D_{\max}$ distributions, since the smallest change in the FSD after a ~~break-up~~ fragmentation event

results in a change of $D_{\max,\mathrm{LIM3}}$. Values between 0.5 and 0.8 lead to smoother FSDs, but overall the choice of $k_{D_{\max}}$ does not significantly affect our results. In the following, $k_{D_{\max}}$ is set to 0.5.

Floes that have never been broken by waves have no physical reason to follow this truncated power-law. In practice, if we consider a discrete number N of floe size categories, the N^{th} category should represent these unbroken floes, with a different condition to set the value of $D_{\max,\mathrm{LIM3}}$ to D_N (the upper size limit of this category). We thus consider ~~that~~ sea ice in a grid cell ~~can be qualified~~ as unbroken only if most of its floes belongs to this N^{th} category, so that $D_{\max,\mathrm{LIM3}} = D_N$ only if $g_N > 0.5c$, g_N being the value of the FSD function associated to the N^{th} category and c the total sea ice concentration.

In all of our simulations, sea ice is initialized as unbroken everywhere, so that $g_N = c$, and $D_{\max,\mathrm{LIM3}} = D_N$. As soon as wave-induced ~~break-up~~ fragmentation occurs, $D_{\max,\mathrm{LIM3}}$ is updated. To do so, the received value of $D_{\max}$ is rounded up to the upper limit of the category it lies in. $D_{\max,\mathrm{LIM3}}$ is therefore slightly greater than the value received from WW3, with an error that depends on the width of its associated floe size category.

Tests ~~on~~ with the simplified domain were also performed with different number and width of floe categories to investigate the sensitivity of the results to ~~the number and width of floes categories~~those parameters. This sensitivity remains really small as long as the widths of the categories are smaller than 10 m and ~~that~~ the categories cover a range of floe sizes larger than 300 m. In the following, we ~~used $N = 60$~~ use $N = 60$ floe size categories, that we define ~~following the conditions~~as follows:

- A first category corresponding to the sea ice floes that are already broken but cannot be broken anymore [$D_0 = 8$ m, $D_1 = 13$ m]. D_0 represents the smallest floe size possible in the model, and is set to 8 m in order to agree with the minimum floe size used in LIM3 to estimate lateral melt from the ~~parameterization~~ formula by Lüpkes et al. (2012). D_0 is also of the same order ~~than~~ as the size of the smallest floes that can be generated by wave-induced ~~break-up (Toyota et al., 2011) and therefore~~ fragmentation (Mellor, 1986) and therefore is an acceptable value for the lower limit $D_{\min}$ that the truncated power-law is assumed to follow after wave-induced ~~break-up~~fragmentation.
- 58 categories for which $D_n - D_{n-1} = 5$ m, with $1 \leq n \leq N - 1$.
- A last category representing unbroken floes [$D_{N-1} = 298$ m, ~~$D_N = 1000$~~$D_N = 1000$ m]. This value of ~~1000 m was~~ $D_N = 1000$ m is set as it is one order of magnitude higher ~~that~~ than the floe size generated by waves (Toyota et al., 2011).

We evaluate the effect of this part of the coupling between WW3 and LIM3, as well as the robustness of the implementation of the FSD in LIM3, by ~~performing~~ looking at the same 2 simulations in our idealized configuration ~~, based on~~ as presented in Fig. 1, and comparing an uncoupled WW3 ~~only or the~~ simulation with a coupled WW3-LIM3 ~~model~~ simulation (Fig. 3). ~~Thermodynamics is still~~ Sea ice thermodynamics are switched off in the WW3-LIM3 simulation. In the uncoupled WW3 simulation, $D_{\max}$ evolves depending on the sea state, but sea ice thickness and concentration are constant. In the WW3-LIM3 coupled simulation, sea ice properties are all evolving as sea ice is pushed by the WRS, and $D_{\max}$ is advected with the FSD

in LIM3. The comparison between $D_{\max}$ estimated from the WW3 simulation and $D_{\max,\mathrm{LIM3}}$ from the coupled ~~framework is shown on~~ simulation is shown in Fig. 3(a,b,c). The pattern of broken sea ice is broadly similar in the two simulations (a,b), despite the sea ice retreat due to the WRS in the coupled case. Differences in $D_{\max}$ (Fig. 3c) follow the wave ~~heights~~ height differences already commented on in Fig. 1(e,f). Indeed, the retreat of the ice edge due to the WRS allows for waves to propagate further with less attenuation, thus involving more sea ice ~~break-up~~ fragmentation and a lower maximum floe size close to the open ocean in the coupled simulation. Further east in the MIZ, the sea ice compacted by the WRS effect generates stronger wave attenuation, and thus less sea ice fragmentation and a ~~greater maximum floe sizes~~ larger maximum floe size when compared to the ~~not-coupled~~ uncoupled simulation. Both effects partly compensate, so that the shift in the ice edge position ~~affects very little the~~ has little effect on the spatial extent of broken ice~~, which is almost unchanged between the two simulations~~. Fig. 3d shows the FSD at two locations in the domain. At both locations, the distribution of ~~ice covered~~ ice-covered area within the different categories agrees very well between LIM3 and the truncated power-law assumed in WW3. The area covered by floes of the smallest possible size in LIM3 is nevertheless greater than it would be if the FSD was exactly following the truncated power-law. This is because floes that have been broken ~~to~~ down into the smallest possible size do not contribute to the redistribution (see section A) and accumulate in this category since no lateral growth occurs. Note that a coupled simulation in which advection had been deactivated was also run to ensure that, in a case with unaffected initial sea ice properties, no significant discrepancies were noticeable for both significant wave height and maximum floe size between ~~an coupled and a not-coupled~~ a coupled and an uncoupled simulation (not shown).

3.3 Lateral melt

A parameterization to account for the sea ice lateral melt is already implemented in LIM3. Its formulation follows Steele (1992):

$$\frac{dc}{dt} = -w_{\mathrm{lat}} \frac{\pi}{\alpha \langle D \rangle} c, \tag{9}$$

where c is the sea ice concentration, w_{lat} is ~~a~~ the lateral melt rate, which depends on the difference between sea ice and sea surface temperatures taken from Maykut and Perovich (1987), and α is a coefficient which varies with the floe geometry. By default, $\alpha = 0.66$, which is the average value of the non-circularity of floes obtained by Rothrock and Thorndike (1984). By default, $\langle D \rangle$, which represents the average floe size~~(referred to as the caliper diameter). Based on an number of observations, Lüpkes et al. (2012) fitted a relationship between $\langle D \rangle$ and sea ice concentration, so that the lateral melt in the model can be estimated depending only on~~ , is a function of the sea ice concentration ~~.~~ obtained empirically from observational data by Lüpkes et al. (2012):

$$\langle D \rangle = D_{\min} \left(\frac{c*}{c* - c} \right)^{\beta} \tag{10}$$

where $\beta = 1$ and $c*$ is introduced to avoid a singularity at $c = 1$ and is defined as:

$$c* = \frac{1}{1 - (D_{\min}/D_{\min})^{1/\beta}} \tag{11}$$

This relationship finds a value of $\langle D \rangle$ that increases very little from its minimum value (set to D_0) as long as the sea ice concentration remains lower than $\simeq 0.6$ (see Fig. 3 from Lüpkes et al., 2012). ~~It might be a problem far from the ice edge, where divergence can make the ice concentration decreasing to 0.6 or below with an actual floe size being much greater than $\simeq$ 10 m.~~ In the following, we refer to this lateral melt parameterization as the parameterization of Lüpkes et al. (2012), although we acknowledge that the work of Lüpkes et al. (2012) only provides a relationship between the average floe size and the sea ice concentration.

In the case of our coupled model, we estimate a FSD, and ~~it thus~~ thus it makes sense to implement a parameterization of the lateral melt that depends explicitly on the FSD rather than ~~the~~ on sea ice concentration. Following the work by Horvat and Tziperman (2015) and Roach et al. (2018), we estimate the lateral melt as:

$$\frac{dc}{dt} = \int_0^\infty \Phi_{th} dD = \int_{0^+}^\infty -w - 2w_{\mathrm{lat}} \left(-\frac{\partial g_D}{\partial D} + \frac{2}{D} g_D \right) dD \tag{12}$$

where Φ_{th} is the change in area covered by floes of a size D due to lateral melt (see Eq.7). Note that lateral melt for floes in the unbroken category is computed assuming that all the floes have a size D of 1000 m. Note also that Horvat and Tziperman (2015) and Roach et al. (2018) are considering floe radii in their study, while we are working with floe diameters (hence adding a factor of 2 in Eq.12).

We run two simulations, in which the lateral melt is either estimated from the formulation of Lüpkes et al. (2012), or by our new formulation, which accounts for the ~~actual~~ FSD that is determined by both the sea ice and the wave models (Fig. 4). Here we only activate the lateral melt, and turn off the basal and surface melt. The sea surface temperature is set constant to $T = 0.3^o C$. Floe size categories are the same as in section 3.2. In the case of the Lüpkes et al. (2012) parameterization (Fig. 4a), ~~the~~ lateral melt only depends on the sea ice concentration and thus ~~follow~~ follows its distribution. In the second case (Fig. 4b), lateral melt is highly constrained by both the distribution of the sea state and ice properties, and is only significant where the sea ice is broken. Melt rates are overall higher when estimated from the Lüpkes et al. (2012) parameterization, mostly due to the fact that the average floe size in the ~~non coupled~~ uncoupled run is very close to D_0 for a wide range of concentrations. Unlike the parameterization that we propose here, the parameterization of Lüpkes et al. (2012) results in a significant lateral melt far from the ice edge, where sea ice is mostly compact and unbroken, which is likely unphysical.

4 ~~Importance of wave-sea ice interactions.~~

We find that the results are also sensitive to the choice of D_{min}, regardless of the parameterization used. In the case of our FSD, the sensitivity arises from the use of D_{min} to compute the average diameter of the smallest floe size category, which is the category most affected by lateral melt. In order to quantify the sensitivity to the choice of D_{min}, we run similar experiments to the one presented in Fig.4, varying this time the value of D_{min} (Fig. 5). When using the parameterization of Lüpkes et al. (2012) (Eq. 10 and 11), the volume of sea ice melted laterally roughly doubles when D_{min} is divided by 2

compared to the reference simulation (using $D_{\min}$ = 8 m). In the case of our FSD, the sensitivity is still large but greatly reduced, with an increase of only 20% in response to the same change of $D_{\min}$. Figure 5 also illustrates the strong differences in melted volume between the two parameterizations, with much less lateral melt when computed using the FSD developed here.

4 Importance of wave-sea ice interactions

In this section we compare the three simulations performed with the CREG025 configuration described in Section 2.2, in order to quantify the impact of the ~~including the wave-sea ice interactions for the waves~~coupling on wave, sea ice and ocean surface properties. ~~Remember that although the coupling is only between the wave and the sea ice components, our coupled model includes an ocean component, which is only interacting with the sea ice model but not the wave model. This means that we only consider here the impact that waves may have on the ocean through their impact on the sea ice conditions.~~

To evaluate the impact of waves in the MIZ, we first need to define the MIZ in our model. Various criteria, relying either on sea ice concentration, floe size or the region where waves impact the sea ice floe size, have been previously used to delimit the MIZ (see for instance Dumont et al., 2011; Strong and Rigor, 2013; Sutherland and Dumont, 2018). Here we take the following definition based on the maximum floe size: $0 < \langle D_{\max} \rangle < 700$ m, where ~~$< \langle D_{\max} \rangle$~~ $\langle D_{\max} \rangle$ is the average of the maximum floe size over the ~~studied~~ study period. Physically, it roughly corresponds to the region where sea ice has been broken during a time period that is long enough for the ~~averaged~~ average maximum floe size to ~~be~~ become under 1000 m (which is the limit between the broken and unbroken ice). Note that our results are not dependent on the definition of the MIZ.

4.1 Effect of the coupling at the pan-Arctic scale

4.1.1 Impact on the wave properties

First, we examine the ~~significant wave height H_s in~~ differences between the CPL and WAVE simulations, corresponding respectively to the coupled WW3-LIM3 run and a run performed with WW3 in stand-alone mode forced with sea ice properties from NOT_CPL. When looking at the differences in significant wave height H_s (Fig. 6~~(b,e)). Differences in H_s between the two simulations~~ b), we find that they are small, not exceeding $\simeq$ 15 cm on average. Moreover, the two runs exhibit similar patterns of $D_{\max}$, indicating that the wave-induced ~~break-up~~ fragmentation is similar in the two simulations (Fig. 6~~f~~d). Locally, in the Barents and Greenland seas for instance, the differences ~~of~~ in $D_{\max}$ can be significant, due to the specific ice drift conditions in these regions. Indeed, the overall southward drift of sea ice tends to bring unbroken sea ice from the central Arctic to regions where sea ice is broken up, increasing $D_{\max}$ in the CPL simulation. The signs of the differences in H_s and $D_{\max}$ vary regionally. This might be due to the differences in sea ice concentration and thickness, as the wave attenuation in sea ice is very sensitive to sea ice properties (see for instance Ardhuin et al., 2018). ~~Indeed~~Certainly, the pattern of the differences in H_s between the CPL and WAVE runs is consistent with the differences in sea ice concentration and thickness between the CPL and the NOT_CPL simulations (Fig. 7)~~. One should keep in mind that the sea ice conditions from the NOT_CPL run are used~~

~~as forcing for the WAVE run)~~, with higher waves found in regions where ice is less concentrated and thinner.

4.1.2 Impact on the sea ice and sea surface properties

We now focus on the effect of adding a wave component ~~for~~ on the sea ice properties, by comparing results from the CPL and NOT_CPL simulations. Fig. 7 shows the ~~Pan-Arctic~~ pan-Arctic distribution of the sea ice thickness and concentration averaged over the 37 days considered in the CPL simulation, as well as the differences with the NOT_CPL simulation. These differences are concentrated in the vicinity of the ice edge and ~~exhibits~~ exhibit different signs depending on the location. Positive and negative anomalies tend to compensate, resulting in weak overall ~~difference~~ differences in sea ice extent and volume when averaging over the full Arctic Basin. If we only consider the MIZ, the sea ice volume and area decrease by about 3% and 2%, respectively, between CPL and NOT_CPL (Fig. 8b). Locally, however, these variations can be much larger. In the MIZ of the Beaufort Sea for instance, the relative changes can be as high as 10% for ~~mean sea ice~~ grid cell-average thickness.

There are also ~~difference~~ differences in sea surface properties between the two simulations (Fig. 9), with ~~an average increase~~ average increases in sea surface temperature (SST) and salinity (SSS) in the MIZ ~~of the order~~ as high as 0.5^oC and 0.8 psu locally, respectively. It is worth noting that, in contrast to the sea ice properties, the sign of the differences in SST and SSS tends to be positive, i.e. warmer and saltier in the CPL experiment compared to the NOT_CPL one.

4.1.3 Thermodynamical effect of the coupling

Given that there is no coupling between the ocean and the wave components, the difference in sea surface properties must arise from variations in sea ice conditions, and in particular the sea ice melt, ~~that we investigate~~ and we now investigate this further. Fig. 10(a,b) shows the total sea ice volume ~~melted laterally during the studied~~ loss from lateral melt during the study period in the CPL run as well as ~~its difference with~~ the difference between this and the same quantity from the NOT_CPL run. The sea ice volume melted by lateral melt shows very similar spatial patterns ~~between~~ in the two simulations, although it is estimated from two very different parameterizations (Eq. 9 and Eq. 12), although lateral melt estimated by the parameterization from Lüpkes et al. (2012) tends to be ~~larger in NOT~~ lower in CPL. The difference is substantial, the sea ice volume melted in the MIZ in ~~NOT~~ CPL being 30% ~~larger than in CPL (~~lower than in NOT_CPL (Fig. 8a). Another signal is found in the central Arctic, ~~where the value of lateral melt in the NOT_CPLrun are small but positive. This is due to the~~ while no lateral melt occurs in this region in CPL. This signal actually arises from the combination of the drop in sea ice concentration that happens in the region in August 2010 (Zhao et al., 2018), ~~resulting in a reduction of the average floe size~~ and the use of the parameterization by Lüpkes et al. (2012) to estimate floe size and resulting lateral melt in NOT_CPL. Indeed, lower sea ice concentration values corresponds to estimated average floe sizes below 100 m when estimated ~~by the formulation of Lüpkes et al. (2012)and thus triggering~~ from the parameterization by Lüpkes et al. (2012), and thus some lateral melt is triggered. In contrast, the absence of waves in the middle of the sea ice pack in ~~the coupled simulation results in unbroken ice~~

CPL leaves sea ice unbroken in this region, ~~and therefore no lateral melt~~ preventing lateral melt from occurring. An average floe size of $\simeq$ 100 m in the middle of the pack seems somewhat unrealistic, and highlights the ~~limitation of the parameterization of Lüpkes et al. (2012) when used in Pan-Arctic configurations. This lateral melt enhancement~~ limitations of estimating the floe size using Lüpkes et al. (2012) parameterization in pan-Arctic configurations. Absence of lateral melt in the central Arctic in ~~the NOT_CPL simulation amplifies the decrease of sea ice concentration in this region. The combination of the sea ice concentration decrease and lateral melt in the NOT_CPL simulation therefore explains the deficit~~ CPL explains the excess in sea ice concentration ~~reported in the central Arctic~~ when compared to the ~~coupled~~ uncoupled simulation (Fig. 7b). Moreover, the fact that differences in lateral melt between the two simulations ~~being mostly negative ,~~ are mostly negative means that it cannot explain the regional patterns found in the distribution of sea ice ~~properties~~ property differences.

Fig. 10(c,d) shows the differences in bottom and total ice melt, between the CPL and NOT_CPL simulations. The spatial ~~pattern~~ distributions of the differences in bottom and total ice melt are very similar, meaning that the variations in bottom melt dominate the differences in sea ice melt between CPL and NOT_CPL, although the bottom melt is computed the same way in the two simulations. This result is confirmed by rerunning a coupled and an uncoupled simulation of NEMO-LIM3 while de-activating lateral melt (not shown), which yields differences in total melt distribution almost identical to the ones presented ~~on~~ in Fig. 10(c,d).

The total melted sea ice volume~~melted ,~~ once integrated over the MIZ, increases by 3% between CPL and NOT_CPL, mainly due to the larger volume of sea ice melted laterally in NOT_CPL (Fig. 8a). In parallel, bottom melt slightly decreases by $\simeq$1% between these two simulations. This result ~~does not reflect~~ masks the fact that the regional differences of total melt are dominated by bottom melt. An explanation is that bottom and lateral melt ~~depend both~~ both depend on the available heat in the surface layer, either directly for bottom melt, or indirectly through lateral melt that depends on the SST. If lateral melt occurs, it removes heat from the surface layer, therefore reducing the bottom melt capacity. ~~Oppositely~~Conversely, if this heat is not used for lateral melt, it remains available for bottom melt. The overall decrease of bottom melt in the MIZ between CPL and NOT_CPL visible ~~on~~ in Fig. 8a therefore mostly results from the compensation of the increase of lateral melt due to the change of parameterization, as can be seen ~~on~~ in Figs. 10b and 10c. ~~Actually, in contrast to what was found in previous studies by Zhang et al. (2016); Bennetts et al. (2017); Roach et al. (2018), de-activating completely~~ This compensation mechanism is also reported by Roach et al. (2018) and Bateson et al. (2019) who compare two runs of the sea ice model CICE, one with the standard lateral melt parameterization using a constant floe size of 300 m and one using a FSD (allowing floes smaller than 300 m). In our case, this compensation is strong enough, and completely de-activating lateral melt in both runs ~~(not shown)~~ has a negligible effect on the quantity of melted ice in our simulations~~(not shown)~~.

4.1.4 Dynamical effect of the coupling

The differences in lateral melt between the CPL and the NOT_CPL runs cannot explain the differences in sea ice and sea surface properties seen ~~on~~ in Figs. 7 and 9. We thus investigate the impact of the WRS on the sea ice conditions and melt.

Fig. 10(e,f) show the mean directions of the wind stress and the WRS in the CPL simulation and the ratio of WRS magnitude ~~on~~ to wind stress respectively. This ratio is generally low, not exceeding 15% of the wind stress in the eastern Barents Sea, where the WRS reaches its highest magnitude. This is much smaller than the values retrieved from satellite observations in the Southern Ocean, where the wind stress and the WRS can be of comparable ~~magnitudes~~ magnitude (Stopa et al., 2018a). It is also worth noting that the regions where this relative importance of the WRS compared to the wind is large do not always coincide with regions where differences in sea ice properties are significant (Fig. 7). In the Beaufort Sea for instance, there is substantially less sea ice melt in the CPL simulation than in the NOT_CPL one, although the ratios of WRS over the wind stress are only of the order of a few ~~percents~~ percent (Fig. 10f). The opposite situation is visible in the Barents Sea, where the high relative influence of the WRS does not result in a significant increase of the sea ice melt when the effect of the waves is included. Therefore, ~~the amplitude~~ there is no direct relationship between the intensity of the WRS ~~alone does not allow to conclude on the mechanism through which the WRS impact sea ice melt~~and the differences in sea ice and sea surface properties between the coupled and uncoupled simulations. In the Southern Ocean, Stopa et al. (2018a) found that the orientation of the WRS, ~~that~~ which tends to be orthogonal to the sea ice edge, might explain why WRS ~~might be~~ is as important as the wind (that tends to vary ~~much more its direction~~ in direction much more over time) ~~to determine~~ in determining the position of the sea ice edge. Similarly, here, we found that the WRS is very often orientated orthogonally to the ice edge, towards packed ice. ~~It~~ This is due to the fact that the longer waves encounter sea ice on their path, the more they are attenuated. The direction of propagating waves at a given point in sea ice is then generally imposed by the waves that have ~~traveled~~ travelled the shortest distance in sea ice. This is particularly visible in some ~~part~~ parts of the Greenland and ~~the~~ Kara seas, where wind and wave stresses have opposite ~~direction~~ directions on average. In the Chukchi and the eastern Beaufort seas, the WRS is orthogonal to the wind stress. In contrast, in the Laptev ~~sea~~Sea, the directions of the WRS and the wind stress roughly align, and thus ~~play~~ work together in setting the position of the sea ice edge in the CPL run. However, at the pan-Arctic scale, there is no clear relationship between the WRS direction and the differences in sea ice melt induced by the WRS in the CPL simulation.

The primary effect of the WRS is to push sea ice, modifying the intensity and the direction of the sea ice drift. This impact is significant in the MIZ, where the ~~averaged~~ average sea ice drift velocity increases by $\simeq$9% between the CPL and the NOT_CPL runs (Fig. 8b). This overall increase of the sea ice velocity can be explained by the fact that both WRS and sea ice drift have a dependency on wind direction. As ~~it~~ was the case for sea ice thickness and concentration, the distribution of the differences in sea ice drift velocity between the two simulations varies strongly depending on the region considered (not shown), but exhibits no clear relationship at the ~~Pan-Arctic~~ pan-Arctic scale that could explain the differences in sea ice melt induced by the WRS.

In the following we investigate in further ~~details~~ detail the wave-sea ice interactions in two regions during storms. Indeed, although the differences between the CPL and NOT_CPL run at the pan-Arctic scale ~~remains~~ remain small, it is clear that the way the waves can influence the sea ice and the ocean surface would depend on the local properties of ~~wave~~the waves, wind, sea ice and ocean surface.

4.2 Regional impacts of ~~waves-sea~~ wave-sea ice interactions during storm events

4.2.1 Case 1: Storm in the Beaufort Sea (16-17 August 2010)

We first focus on a storm event that occurred near the MIZ in the Beaufort Sea on 16-17 August 2010 (Figs. 11(a,b,c) and 12(a,e)). During the storm, waves and winds are oriented ~~toward the North-West on the West~~ towards the north-west on the west side of the domain, but ~~toward the West on the East~~ towards the west on the east side. Wave height and wind speed are reaching up to 3 m and 12 m/s (Fig. 11a,b), respectively, while they do not exceed 1 m and 7 m/s during the 3 days preceding the storm (not shown). Before the event, the south Beaufort Sea is ice-free, and the position of the sea ice edge (defined at the 15% sea ice concentration contour) is highly irregular, with the presence of an ice tongue centered around 72^{o}N and 155^{o}W, that is exposed upwind ~~(and waves)~~ on its eastern side but downwind on its western side during the storm. This sea ice tongue is composed of relatively thick ice (~~$\geq 1m$~~ $\geq$ 1m). During the storm, sea ice breaks all over the ice tongue in the western part of the domain, but not further than $\simeq$40 km after the sea ice edge. Both the waves and the wind stresses push the ice to the west (Fig. 11b,c), accelerating the drift that is directed north-west (Fig. 12a,c), as ~~it~~ was already the case before the storm (not shown). The wave action is particularly effective at the location of the sea ice tongue, where the WRS has an amplitude comparable to the wind stress over sea ice (Fig. 11c). As a consequence, the sea ice drift is substantially accelerated (Fig. 12c). ~~Considering the~~ The effect of the waves results in large changes of the sea ice thickness pattern (when comparing the CPL and NOT_CPL runs), with a decrease on the eastern part of the tongue but an increase on the western part (Fig. 12g). Outside of the sea ice tongue, the differences between the simulations are very small, likely because of the sharp sea ice thickness gradient opposing internal resistance to deformation (Fig. 12e), and the relative small effect of the WRS compared to the wind stress (Fig. 11c).

The differences ~~of~~ in sea ice properties around the sea ice tongue between the two runs also result in changes in SST and SSS, with ~~increase~~ increases around 1^{o}C and ~~1psu~~1 psu, respectively, on the eastern side of the sea ice tongue, and a decrease of roughly the same magnitude on the western side (Fig. 13c,g). ~~This differences arises~~ These differences arise from changes in sea ice melt, as differences ~~of~~ in the total heat flux at the sea surface (Fig. 14a) are largely determined by bottom melt (Fig. 14b), the lateral melt contribution being one order of magnitude lower in this case. On the eastern side of the sea ice tongue, waves tend to push the sea ice away from the edge in the CPL run, and thus away from surface waters with warmer SST, resulting in a smaller amount of heat in the surface layer available for bottom melt. As the sea ice melt decreases, it also reduces the amount of freshwater received by the ocean surface, resulting in larger SSS. On the western side of the south end of the ice tongue, where the sea ice is thicker in the CPL run than in the NOT_CPL one, the opposite effect happens, ~~eventually~~ explaining the lower SST and SSS values. One should note that the effects of this storm are particularly strong, due to the specific conditions before the storm, with warm waters brought very close to the sea ice edge during the storm (not shown) .

In our model, bottom melt arises from heat fluxes determined by two distinct processes: (i) a conductive heat flux, ~~which intensity~~ the intensity of which is controlled by the difference between sea ice temperature and SST, and (ii) a turbulent heat flux in the surface layer, which depends on both the SST and the shear between the sea ice and the sea surface currents. The inclusion of the ~~effect of the waves and the~~ WRS could in principle ~~modified the total bottom melt~~ affect the turbulent heat flux through its effect on the sea ice drift, but it is not the case here, suggesting that the deficit of sea ice melt on the eastern side of

the sea ice tongue in the CPL run is therefore due to the combination of colder SST and ~~the~~ sea ice reduction.

4.2.2 Case 2: Storm in the Barents Sea (16-17 August 2010)

The storm that we just examined in the Beaufort Sea occurred on the same date ~~than~~ as a second and stronger storm in the Barents Sea, with wave heights up to 5 m and south-westward winds reaching $\simeq$15m/s on average over the two days (bottom panels of Fig. 11d,e). In the CPL run, waves ~~break-up~~ fragments sea ice over a very large area (Fig. 12f). Similarly to what we see in the Beaufort Sea, the mean direction of propagation of the waves aligns with the direction of the wind over the ice-free ocean, and is rotated orthogonally to the gradient in sea ice thickness once in the sea ice pack (Fig. 11d). The transition is however much smoother here than in the Beaufort Sea as the gradient is much weaker (Fig. 12f). In the CPL run, sea ice is drifting southward (Fig. 12b), with a slight deviation from the wind direction, and speeds twice ~~larger than~~ as large as in the Beaufort Sea, due to stronger winds and thinner and less concentrated sea ice.

In contrast to the ~~effect~~ effects of the storm in the Beaufort Sea, the WRS in the CPL run reaches large values (Fig. 11f). Indeed, the strong storm generates ~~very high wavesof which attenuation induces WRS~~ high waves, inducing a WRS as large as the wind stress close to the sea ice edge ~~as large as the wind stress~~where most of the attenuation takes place, although the WRS does not align with the direction of the wave propagation in ice. This is due to the low sea ice concentration in this region that allows for wave generation ~~on~~ over a large region, even if partially ice-covered. The attenuation of these short in-ice generated waves dominates the WRS that is therefore aligned with the wind direction, thus accelerating the ice drift, especially close to the ice edge (Fig. 12d).

The differences in sea ice drift between the CPL and the NOT_CPL runs also result in differences in bottom melt (Fig. 14d), and more specifically ~~of~~ in the part associated with the turbulent heat flux (not shown). This increase of the turbulent heat flux, which occurs in the Barents Sea but not in the Beaufort Sea, can be explained by the larger ice drift velocities driven by the WRS, which intensify the shear between the sea ice and the ocean, and therefore the turbulence in the surface mixed layer. The differences in sea ice drift between the two runs also result in changes of the conductive heat flux. ~~Yet~~However, in the Barents Sea, the sea ice thickness and concentrations are lower than in the Beaufort Sea while the sea ice temperature is ~~overall higher~~ higher overall (not shown). This results in only moderate differences of the conductive heat flux between the CPL and ~~the~~ NOT_CPL runs.

The differences in SST and SSS exhibit similar ~~pattern than~~ patterns to the differences in heat flux (Fig. 13d,h and Fig. 14c), but the magnitude of the differences are much weaker than in the Beaufort Sea, not exceeding a few tenths of ^{o}C and psu for SST and SSS respectively. These small differences can be explained by two causes: (i) the small differences of sea ice properties between the two simulations result in small changes in melt, and (ii) the initial state before the storm is also different with higher SST and SSS in CPL (not shown). This difference in the initial state can be related to previous ~~waves~~ wave and

wind conditions~~(not shown)~~: low wind speeds are not sufficient to generate waves in the MIZ, implying that the WRS must be directed northward in the same direction as the propagating waves. It therefore compacts the sea ice edge, and thus reduces sea ice melt in the MIZ in the CPL run. As seen in the Beaufort Sea case, this in turn leads to higher SST and SSS values in the vicinity of the ice edge.

4.2.3 What determines the impact of the waves?

From these two particular cases we suggest a generalization of the mechanisms by which the waves can impact the sea ice and ocean properties in the MIZ. It is based on a simple principle: if sea ice is moved towards warmer water, it tends to melt more, and *vice versa*. The direction of the WRS compared to the orientation of the sea ice edge is thus fundamental if we are to understand the impact of the waves. In compact sea ice, waves are quickly attenuated and the direction of the WRS is generally towards the packed ice, thus impeding part of the sea ice melt and increasing the SST and SSS (Fig. 9). In regions where the sea ice is less concentrated and thinner, waves can be generated locally, so that the WRS aligns with the wind, whose direction determines the impact of the WRS (enhanced melt for off-ice wind and reduced melt for on-ice wind). Another key factor determining the impact of the WRS ~~onto~~ on sea ice is the internal stress of sea ice (a.k.a the rheology; see Eq.2). The impact of the WRS is larger in regions of the MIZ where the sea ice is thin and ~~low concentrated~~has low concentration, as the internal stress tends to be negligible (Hibler III, 1979), making the sea ice easier to deform and to drift freely. Close to the sea ice edge in the Barents Sea for instance, the WRS in storm-induced high ~~waves~~ wave conditions can be larger than the wind stress, strongly accelerating the sea ice drift towards the open ocean, which also ~~result~~ results in an increase of the ~~ice/ocean~~ ice-ocean shear, enhancing the turbulent heat flux under sea ice and thus the sea ice melt.

5 Discussion and conclusion

The goal of this study was to examine the wave-sea ice interactions in the MIZ of the Arctic Ocean during the melt season, as these processes are thought to be important for determining the sea ice conditions but are not accounted for in the state-of-the-art sea ice models. To that aim, we have developed a model framework, coupling the wave model WW3 with a modified version of the ocean/sea ice model NEMO-LIM3. The coupled model was then used to examine two aspects of the wave-sea ice interactions: (i) the impact of the WRS on the sea ice drift in the MIZ, and (ii) the effects of using the wave-induced sea ice ~~break-up on the sea ice~~ fragmentation to estimate lateral melt. The WRS tends to compact the ice edge and thus reduces the total sea ice melt in the MIZ. Yet, its overall impact on the MIZ sea ice area and volume remains limited (Fig. 8b). However, it has a visible impact on sea ice drift velocity, accelerating it by $\simeq$9%. Compared to the use of ~~Lüpkes et al. (2012) parameterization~~ the parameterization of Lüpkes et al. (2012) to estimate the floe size used in lateral melt, our parameterization strongly reduces the amount of sea ice melted laterally. It is however mostly compensated by an increase of bottom melt, similar to what was found by Bateson et al. (2019). As a result, the effects on sea ice and sea surface properties can be locally substantial, and even more substantial during storms, as illustrated by the case studies in the Beaufort and Barents seas. As the storminess in

the Arctic region is expected to increase in the future (Day et al., 2018; Day and Hodges, 2018), generating higher and more energetic waves more frequently (Khon et al., 2014), the wave-sea ice interactions might become a dominant signal controlling the dynamics of the MIZ.

In the MIZ, waves push sea ice as they are attenuated, ~~modifying locally~~ locally modifying the position of the sea ice edge through a modulation of the magnitude and timing of the sea ice melt, which ~~result~~ results in significant changes of the SST and SSS. Although the impact at the pan-Arctic scale remains limited, the case studies of storms in the Barents and Beaufort seas ~~shows that it~~ show how this modulation can be locally and intermittently important. Results from our simple configuration have also revealed that the WRS could strongly modulate the position of the sea ice edge. Yet, except very locally in response to strong storms, the position of the pan-Arctic sea ice edge simulated by our realistic configuration appears to be insensitive to the effect of the wave. This is likely because the position of the sea ice edge in a ocean-sea ice model is primarily determined by the atmospheric forcing and the bulk formulae, and is in particular strongly ~~tight~~ tied to the position of the sea ice edge in the atmospheric reanalysis (Chevallier et al., 2017). The ~~effect~~ effects of the waves on sea ice simulated by our coupled model are likely underestimated, and should be re-assessed in future studies based on a fully coupled model that includes an atmospheric component.

We ~~also have~~ have also tested two parameterizations of the lateral melt, based either on wave-induced ~~break-up~~ fragmentation information or solely on a scaling between the size of the floes and the sea ice concentration, following Lüpkes et al. (2012). ~~In both cases, the~~ We first acknowledge that the effect of our lateral melt parameterization depends strongly on the FSD, and hence on the choices and assumptions made regarding its implementation. For instance, our redistribution scheme associated with sea ice fragmentation assumes that successive fragmentation events lead to a power-law FSD. This assumption is made based on the observations analyzed by Toyota et al. (2011), that only sample a small area in time and space, and their findings may not be applicable globally. More generally, Roach et al. (2018) recommend avoiding forcing the shape of the distribution, as the analysis of observations have revealed that FSDs do not always follow power-law distributions (e.g. Inoue et al., 2004). They foster the use of alternative approaches, such as the one developed by Horvat and Tziperman (2015). However, results from laboratory experiments focusing on the fragmentation of sea ice by waves by Herman et al. (2018) indeed suggest power-law distributions for the smallest floe sizes generated, similarly to what was found by Toyota et al. (2011) for the small floes regime. This justifies the choice made in the present study. More generally, large uncertainty remains regarding the key parameters governing the FSD redistribution (coming from waves or sea ice properties), and more dedicated observations will be needed in the future to better constrain FSD in models.

Regardless of the choices made for the implementation of the FSD, the effect of the lateral melt for both formulations remains limited as any change of lateral melt tends to be compensated by an opposite change of bottom melt. The effect might however become more important if longer simulations were performed. Indeed, Zhang et al. (2016) found that, over a year, the lateral melt could ~~affect significantly~~ significantly affect the sea ice thickness. In their case, a FSD-based parameterization

was used (similar to the one we introduced in our coupled model), but the effect of the wave-induced ~~break-up~~ fragmentation on the FSD was only crudely parameterized, resulting ~~in~~ most likely in an overestimation of lateral melt in the central Arctic ~~most likely over-estimated~~ (as this is the case when using the parameterization of Lüpkes et al., 2012). Adding a FSD in their sea ice model, ~~? found~~ Roach et al. (2018) found a large impact on ~~the~~ sea ice concentration in the MIZ and sea ice thickness everywhere in the Arctic after 20 years of simulation, and suggested that the ~~difference~~ differences found in the central Arctic ~~results~~ result from a redistribution of the heat used for lateral melt instead of bottom melt, similar to what happens in our model over a shorter timescale. One should also remember that the studies of Zhang et al. (2016) and ~~? were aiming at representing~~ Roach et al. (2018) aimed to represent the evolution of floes ~~larger than 1000 m~~ with sizes ranging from a few cm to roughly 1 km on long time scales, whereas we focus on the important processes for wave-sea ice interactions and make the assumption that unbroken floes have ~~an~~ a uniform floe size set to 1000 m~~in order to focus on the important processes for the wave-sea ice interactions~~. Therefore we do not expect any impact of the lateral melt in regions that are not impacted by waves. Note also that we evaluate the impact of changing the lateral melt parameterization by comparing two simulations for which lateral melt depends on a varying floe size, either deduced from the FSD or estimated from the sea ice concentration using the parameterization suggested in Lüpkes et al. (2012). It differs from Zhang et al. (2016) who compare their FSD-model with a reference run without lateral melt, and from Roach et al. (2018) who use a constant floe size of 300 m in their lateral melt parameterization. This might partly explain the discrepancies between our respective conclusions.

Among the wave-sea ice interaction processes considered in this study, we ~~found~~ find that the dynamical effect of the waves (the WRS) has a larger impact ~~than the thermodynamical one (through the additional lateral source melt)~~on sea ice conditions and sea surface properties than the modulation of lateral melt by sea ice fragmentation. Our simulations were however limited to only a few weeks during the melting season and it is unclear if ~~that~~ the result would hold if longer timescales were considered. ~~To make progress on~~ In order to answer this question, we would need to implement a parameterization that ~~account~~ accounts for the refreezing of ~~the~~ floes, through lateral growth and welding. A first parameterization of ~~that~~ this kind has been very recently developed by Roach et al. (2018). We also anticipate that running a simulation over longer time ~~period~~ periods would highlight new impacts of the WRS. Indeed, observations have revealed that heat stored during the melt season below the mixed layer can significantly affect ~~the~~ sea ice growth the following year (Jackson et al., 2010; Timmermans, 2015). In regions where the WRS contributes to ~~reduce~~ reducing the ice melt, an excess of summer heat could likely accumulate under the mixed layer, possibly modulating the future evolution of the sea ice melt and growth. Recently, Smith et al. (2018)~~have for instance~~, for instance, observed that a large amount of heat stored under the mixed layer could be released to melt sea ice during a storm. The significant changes of SST and SSS found locally over 37 days also highlight that wave-sea ice interactions should be considered when trying ~~the~~ to forecast the Arctic sea ice conditions on short ~~timescale~~ timescales (up to a few weeks), as these surface ocean changes can greatly affect melting and refreezing conditions.

The coupling developed in ~~the present~~ this study marks a valuable new step ~~toward~~ towards an improved representation of waves and sea ice interactions in models, which might improve the representation of the dynamics ~~of~~ in the MIZ. Yet, our

coupling relies on a number of assumptions, which are most likely leading to an underestimation of the impact of the ~~wave~~ waves on the ocean and sea ice conditions. For instance, in our coupling, the sea ice rheology is unaffected by fragmentation, which is unlikely to be the case in reality (McPhee, 1980). Moreover, the sea ice model used here does not retain any memory of the past sea ice conditions, while ~~wave~~ waves would most likely ~~affect differently~~ have a different effect on sea ice that has been previously broken (Langhorne et al., 1998). Developing a similar coupling using a model that ~~consider~~ considers a state variable accounting for the previous sea ice conditions (such as ~~the state variable 'damage' included in the~~ in the neXtSIM sea ice model ~~neXtSIM~~ (Rampal et al., 2016; Williams et al., 2017)) would probably reveal new mechanisms via which waves can modulate the ocean and sea ice conditions in the MIZ.

Finally, the coupling we have developed here is also only considering the interactions between ~~wave~~ waves and sea ice, without any direct coupling with the ocean and the atmosphere. Yet, we know that wave dissipation would also likely impact the mixed layer, by enhancing turbulence (Couvelard et al., Submitted), and eventually modulate the rate of sea ice melt and formation (Martin and Kauffman, 1981; Rainville et al., 2011; Lee et al., 2012; Smith et al., 2018). Similarly, the effect of the waves is probably damped due to the lack of feedbacks with the atmosphere (Khon et al., 2014). Future coupling should include some of these features in order to fully capture the complexity of the MIZ dynamics.

Code and data availability. Will be made available before final submission

Appendix A: Floe size redistribution in the sea ice model LIM3

Here we provide the details of the calculation and implementation of the FSD, and in particular of the mechanical redistribution function Φ_m that accounts for processes such as sea ice fragmentation, lead opening, ridging, and rafting. Following Zhang et al. (2015), Φ_m can be divided into 3 terms as $\Phi_m = \Phi_o + \Phi_r + \Phi_f$ where Φ_o represents the creation of open water, Φ_r represents sea ice ridging and rafting, and Φ_f represents the wave-induced ~~floes~~ floe fragmentation. Here we compute Φ_o and Φ_r in a similar way to Zhang et al. (2015), assuming that all the floes of different sizes have the same ice thickness distribution, so that changes in sea ice concentration due to open water creation or ridging ~~affects~~ affect all floes equally. As a result, the shape of the FSD and its evolution are independent from these two terms.

Assuming that, in a given grid cell, sea ice fragmentation does not induce any change of the sea ice concentration, Φ_f can be written as (Zhang et al., 2015):

$$\Phi_f = -Q(D)g_D(D) + \int_0^\infty Q(D')\beta(D', D)g_D(D')dD' \tag{A1}$$

where D is the floe size, $Q(D)$ is a redistribution probability function characterizing which floes are going to be broken depending on their size, and $\beta(D', D)$ is a redistribution factor quantifying the fraction of sea ice concentration transferred from one floe size to another as ~~break up~~ fragmentation occurs. Φ_f is thus used to transfer sea ice concentration from large

floes to smaller floes. To ensure the conservation of sea ice area during fragmentation, β must respect (Zhang et al., 2015):

$$\int_0^\infty \beta(D', D) dD = 1 \tag{A2}$$

In the absence of a wave model to simulate the sea state, Zhang et al. (2015) ~~has~~ defined β so that it ~~redistributes uniformly~~ uniformly redistributes the sea ice concentration of the large broken floes into the smaller floe ~~sizes~~ size categories of the FSD. Their redistribution probability function $Q(D)$ thus assumes that a constant fraction of the sea ice cover is broken by waves during each ~~break-up~~ fragmentation event. Their definition of $Q(D)$ also ensures that larger floes contribute more to the redistribution than smaller floes.

In our coupled model, sea ice ~~break-up~~ fragmentation is initially computed by WW3 (for details see Boutin et al., 2018), and accounts for the sea state variability. In WW3, the FSD resulting from wave-induced ~~break-up~~ fragmentation is assumed to follow a truncated power-law between a minimum ($D_{\min}$) and a maximum ($D_{\max}$) floe size. For consistency, the FSD in LIM3 after a given ~~break-up~~ fragmentation event must follow the same power-law, defined for D taken in $[D_{\min}\ D_{\max}]$ ~~as~~such as, for a given floe size D_* also taken in $[D_{\min}\ D_{\max}]$:

$$P(D > D_*) = K D_*^{-\gamma}, K \in \mathbb{R} \tag{A3}$$

$$p(D) = -K\gamma D^{-\gamma-1} \tag{A4}$$

where $P(D > D_*)$ is the probability of having $D > D_*$, and $p(D)$ is the associated probability density. In WW3, a ~~break-up~~ fragmentation event occurs if, firstly, waves with a wavelength λ ~~applies~~ apply a strain on sea ice greater than a given threshold, and secondly if $\lambda/2$ which is assumed to be the value of the new maximum floe size is lower than the current $D_{\max}$ value in the wave model (Dumont et al., 2011). Therefore, a ~~break-up~~ fragmentation event in WW3 corresponds to a decrease of $D_{\max}$.

As detailed in section 3.2, we define a maximum floe size in LIM3, $D_{\max,\mathrm{LIM3}}$, that is compared to the value of the maximum floe size received from WW3, $D_{\max,\mathrm{WW3}}$. Initially, ice is unbroken and $D_{\max,\mathrm{LIM3}} = D_{\max,\mathrm{WW3}}$. If ~~break-up~~ fragmentation has occurred in WW3, then we have $D_{\max,\mathrm{WW3}} < D_{\max,\mathrm{LIM3}}$. In this case, $D_{\max,\mathrm{LIM3}}$ must be updated to the $D_{\max,\mathrm{WW3}}$ value, and Φ_f must be computed so that it forces the FSD in LIM3 to match the FSD assumed in WW3.

In practice, in LIM3, we define a given number N of floe size categories, such that each floe size category $n \in [0, N]$ represents the floes with sizes in $[D_{n-1}, D_n]$. D_0 and D_N are the minimum and the maximum floe size possible in the model, respectively. D_N aims ~~at representing~~ to represent floes that have not been broken by the waves. In WW3, the size of unbroken floes is set to 1000 m, and we thus also set D_N=1000m for consistency. Regarding the minimum floe size resulting from wave induced ~~break-up~~fragmentation, we set $D_{\min}$ to 8 m, which is the value of the minimum floe size used in the parameterization of lateral melt implemented in LIM3. This value is close to choices ~~done~~ made in previous studies (see Williams et al., 2013; Bennetts et al., 2017). If ~~break-up~~ fragmentation occurs, the update of $D_{\max,\mathrm{LIM3}}$ is done as follows:

$$\begin{cases} D_{n^*-1} < D_{\max,\mathrm{WW3}} \leq D_{n^*} \\ D_{\max,\mathrm{LIM3}} = D_{n^*}. \end{cases} \tag{A5}$$

Here n^* is the index of the floe size category in which the maximum floe size received from the wave model lies in. $D_{\mathrm{max,LIM3}}$, the maximum floe size in the sea ice model is thus set equal to D_{n^*}, the upper bound of the n^*th category. To force the FSD to follow this power-law during the computation of the mechanical redistribution term Φ_f, in LIM3 we introduce changes in the computation of β and $Q(D)$. When using N floe size categories, the redistribution equation (A1) becomes:

$$\Phi_{f,n} = -Q_n g_n + \sum_{m=1}^{N} \beta(m,n) Q_m g_m \quad , m \in [0, N] \tag{A6}$$

Following Zhang et al. (2015), the redistribution factor $\beta(m,n)$ must respect Eq.A2. $\beta(m,n)$ should also allow ~~to~~ for a switch from completely unbroken ice to a truncated power-law distribution with lower limit D_0 and upper limit $D_{\mathrm{max,LIM3}}$ if ~~break-up occurs.~~ fragmentation occurs. Finally, $\beta(m,n)$ must ~~finally~~ ensure that floe size can only decrease during the fragmentation. To do so, $\beta(m,n)$ is defined as:

$$\begin{cases} \beta(m,n) = \dfrac{D_n^{2-\gamma} - D_{n-1}^{2-\gamma}}{\min(D_{n^*}, D_m)^{2-\gamma} - D_0^{2-\gamma}} \text{ if } m \geq n \text{ and } n \leq n^* \\ \beta(m,n) = 0 \text{ otherwise} \end{cases} \tag{A7}$$

With this choice of $\beta(m,n)$, the FSD of each floe size category $n < n^*$ is equal to the distribution function derived from the power-law assumed in WW3 ($g_{n,\mathrm{P.L}}$), given by:

$$g_{n,\mathrm{P.L}} = c \frac{\int_{D_{n-1}}^{D_n} D^2 p(D) dD}{\int_{D_0}^{D_{\max}} D^2 p(D) dD} = c \frac{D_n^{2-\gamma} - D_{n-1}^{2-\gamma}}{D_{\max}^{2-\gamma} - D_0^{2-\gamma}}, \tag{A8}$$

c being the sea ice concentration.

If sea ice in a given grid cell has already been broken, the FSD may have deviated from the truncated power-law distribution (due to advection or melting). If ~~break-up~~ fragmentation occurs again at a ~~latter~~ later model time step, we force the FSD to be reset to the power-law assumed in WW3, by adjusting the fraction of each floe size category contributing to the redistribution through the value Q_n. This ensures that the FSD in LIM3 and WW3 are identical. After a ~~break-up~~ fragmentation event, $D_{\mathrm{max,LIM3}}$ is the new maximum floe size in LIM3. The sea ice contained in floe size categories associated with floes larger than $D_{\mathrm{max,LIM3}}$ is therefore entirely redistributed into smaller floe size categories by setting:

$$Q_n|_{n>n^*} = 1. \tag{A9}$$

The smallest floe size category (*i.e* $D \in [D_0, D_1]$) does not contribute to the floe size redistribution, assuming that this category accounts for floes too small to be broken by waves (Toyota et al., 2011). It therefore forces $Q_1 = 0$. For a given floe size category n, we define $\Delta g_{th,n}$ as the difference between the actual and theoretical values of the FSD for this floe size category ($\Delta g_{th,n} = g_n - g_{n,\mathrm{P.L}}$), and the theoretical value is given by the truncated power-law between D_0 and $D_{\mathrm{max,LIM3}}$~~)~~. After the redistribution of floes between categories, $\Delta g_{th,n}$ needs to be zero, which is achieved through the adjustment of Q_n in order

to obtain $\Phi_{f,n} = \Delta g_{th,n}$. The following system thus needs to be solved:

$$\begin{cases} \Phi_{f,2} = (-1+\beta_{2,2})Q_2 g_2 + \beta_{3,2} Q_3 g_3 + ... + \beta_{n^*,2} Q_{n^*} g_{n^*} + \sum_{n>n^*}^{N} \beta_{n\geq n^*,2} g_n \\ \Phi_{f,3} = (-1+\beta_{3,3})Q_3 g_3 + \beta_{4,3} Q_4 g_4 + ... + \beta_{n^*,n^*} Q_{n^*} g_{n^*} + \sum_{n>n^*}^{N} \beta_{n\geq n^*,3} g_n \\ ... \\ \Phi_{f,n^*} = (-1+\beta_{n^*,n^*})Q_{n^*} g_{n^*} + \sum_{n>n^*}^{N} \beta_{n\geq n^*,n^*} g_n, \end{cases} \tag{A10}$$

This system consists in a triangular matrix in which all diagonal terms are non-zero. It is solved by doing:

$$\begin{cases} Q_{n^*} = \max\left(0, \dfrac{\Delta g_{th,n^*} - \sum_{n>n^*}^{N} \beta_{n\geq n^*,n^*} g_n}{g_{n^*}(\beta_{n^*,n^*} - 1)}\right) \\ ... \\ Q_2 = \max\left(0, \dfrac{\Delta g_{th,2} - \sum_{n>2}^{N} Q_n \beta_{n,2} g_n}{g_2(\beta_{2,2} - 1)}\right) \end{cases} \tag{A11}$$

The constraint $Q_n > 0$ ensures that the redistribution can only be done ~~toward~~ towards categories containing smaller floe ~~size~~sizes. This constraint thus implies that, in the case where $\Delta g_{th,n} > 0$, the FSD in LIM3 is reset to the truncated power-law only if there is enough sea ice in large ~~floes~~ floe categories to be redistributed into smaller ~~floes~~ floe categories. Besides, setting $Q_1 = 0$ means that the sea ice concentration associated with the smallest floe size category is never redistributed. In the absence of lateral growth, a succession of ~~break-up~~ fragmentation events leads to an accumulation of floes in this category, deviating the FSD from the theoretical power-law for floe sizes between D_0 and D_1 (see Fig. 3).

Competing interests. The authors declare no competing interests.

Acknowledgements. G.B. and F.A. are supported by DGA, ANR grants ANR-14-CE01-0012 MIMOSA, ANR-10-LABX-19-01, EU-FP7 project SWARP under grant agreement 607476, ONR grant number N0001416WX01117. Part of this work has been carried out as part of the Copernicus Marine Environment Monitoring Service (CMEMS) ArcticMix and WIzARd projects. CMEMS is implemented by Mercator Ocean in the framework of a delegation agreement with the European Union. We thank Martin Vancoppenolle for ~~its~~ his valuable help as well as Verena Haid and Xavier Couvelard for their ~~precious~~ significant assistance in setting up the coupled framework.

References

Aksenov, Y., Popova, E. E., Yool, A., Nurser, A. G., Williams, T. D., Bertino, L., and Bergh, J.: On the future navigability of Arctic sea routes: High-resolution projections of the Arctic Ocean and sea ice, Marine Policy, 75, 300–317, 2017.

Ardhuin, F., Sutherland, P., Doble, M., and Wadhams, P.: Ocean waves across the Arctic: attenuation due to dissipation dominates over scattering for periods longer than 19 s, Geophys. Res. Lett., 43, https://doi.org/10.1002/2016GL068204, 2016.

Ardhuin, F., Chapron, B., Collard, F., Smith, M., Stopa, J., Thomson, J., Doble, M., Wadhams, P., Blomquist, B., Persson, O., and Collins, III, C. O.: Measuring ocean waves in sea ice using SAR imagery: A quasi-deterministic approach evaluated with Sentinel-1 and in situ data, Remote Sensing of Environment, 189, 211–222, 2017.

Ardhuin, F., Boutin, G., Stopa, J., Girard-Ardhuin, F., Melsheimer, C., Thomson, J., Kohout, A., Doble, M., and Wadhams, P.: Wave Attenuation Through an Arctic Marginal Ice Zone on October 12, 2015: 2. Numerical modeling of Waves and Associated Ice Break-Up, Journal of Geophysical Research: Oceans, https://doi.org/10.1002/2018JC013784, 2018.

Asplin, M. G., Galley, R., Barber, D. G., and Prinsenberg, S.: Fracture of summer perennial sea ice by ocean swell as a result of Arctic storms, J. Geophys. Res., 117, C06 025, https://doi.org/10.1029/2011JC007221, 2012.

Barnier, B., Madec, G., Penduff, T., Molines, J.-M., Treguier, A.-M., Sommer, J. L., Beckmann, A., Biastoch, A., Böning, C., Dengg, J., Derval, C., Durand, E., Gulev, S., Remy, E., Talandier, C., Theetten, S., Maltrud, M., McClean, J., and Cuevas, B. D.: Impact of partial steps and momentum advection schemes in a global ocean circulation model at eddy-permitting resolution, Ocean Modelling, 56, 543–567, https://doi.org/10.1007/s10236-006-0082-1, 2006.

Bateson, A. W., Feltham, D. L., Schröder, D., Hosekova, L., Ridley, J. K., and Aksenov, Y.: Impact of floe size distribution on seasonal fragmentation and melt of Arctic sea ice, The Cryosphere Discussions, 2019, 1–35, https://doi.org/10.5194/tc-2019-44, https://www.the-cryosphere-discuss.net/tc-2019-44/, 2019.

Bennetts, L., O'Farrell, S., and Uotila, P.: Brief communication: Impacts of ocean-wave-induced breakup of Antarctic sea ice via thermodynamics in a stand-alone version of the CICE sea-ice model, The Cryosphere, 11, 1035–1040, https://doi.org/10.5194/tc-11-1035-2017, 2017.

Bouillon, S., Fichefet, T., Legat, V., and Madec, G.: The elastic–viscous–plastic method revisited, Ocean Modelling, 71, 2–12, https://doi.org/10.1016/j.ocemod.2013.05.013, 2013.

Boutin, G., Ardhuin, F., Dumont, D., Sévigny, C., Girard-Ardhuin, F., and Accensi, M.: Floe Size Effect on Wave-Ice Interactions: Possible Effects, Implementation in Wave Model, and Evaluation, Journal of Geophysical Research: Oceans, 123, 4779–4805, https://doi.org/10.1029/2017JC013622, 2018.

Brodeau, L., Barnier, B., Treguier, A.-M., Penduff, T., and Gulev, S.: An ERA40-based atmospheric forcing for global ocean circulation models, Ocean Modelling, 31, 88–104, 2010.

Cheng, S., Rogers, W. E., Thomson, J., Smith, M., Doble, M. J., Wadhams, P., Kohout, A. L., Lund, B., Persson, O. P., Collins, C. O., et al.: Calibrating a viscoelastic sea ice model for wave propagation in the arctic fall marginal ice zone, Journal of Geophysical Research: Oceans, 122, 8770–8793, 2017.

Chevallier, M., Smith, G. C., Dupont, F., Lemieux, J.-F., Forget, G., Fujii, Y., Hernandez, F., Msadek, R., Peterson, K. A., Storto, A., et al.: Intercomparison of the Arctic sea ice cover in global ocean–sea ice reanalyses from the ORA-IP project, Climate Dynamics, 49, 1107–1136, 2017.

Collins, III, C. O., Rogers, W. E., Marchenko, A., and Babanin, A. V.: In situ measurements of an energetic wave event in the Arctic marginal ice zone, Geophys. Res. Lett., 42, 1863–1870, https://doi.org/10.1002/2015GL063063, 2015.

Comiso, J. C., Meier, W. N., and Gersten, R.: Variability and trends in the Arctic Sea ice cover: Results from different techniques, Journal of Geophysical Research: Oceans, 2017.

Couvelard, X., Lemarié, F., Samson, G., Redelsperger, J.-L., Ardhuin, F., Benshila, R., and Madec, G.: Development of a 2-way coupled ocean-wave model: assessment on a global oceanic configuration, Geoscientific Model Development, Submitted.

Craig, A., Valcke, S., and Coquart, L.: Development and performance of a new version of the OASIS coupler, OASIS3-MCT_3. 0, Geoscientific Model Development, 10, 3297, 2017.

Day, J. J. and Hodges, K. I.: Growing land-sea temperature contrast and the intensification of Arctic cyclones, Geophysical Research Letters, 45, 3673–3681, 2018.

Day, J. J., Holland, M. M., and Hodges, K. I.: Seasonal differences in the response of Arctic cyclones to climate change in CESM1, Climate dynamics, 50, 3885–3903, 2018.

Dumont, D., Kohout, A., and Bertino, L.: A wave-based model for the marginal ice zone including a floe breaking parameterization, J. Geophys. Res., 116, C00E03, https://doi.org/10.1029/2010JC006682, 2011.

Dupont, F., Higginson, S., Bourdallé-Badie, R., Lu, Y., Roy, F., Smith, G., Lemieux, J., Garric, G., and Davidson, F.: A high-resolution ocean and sea-ice modelling system for the Arctic and North Atlantic oceans, Geoscientific Model Development, 8, 1577, 2015.

Feltham, D. L.: Granular flow in the marginal ice zone, Philosophical Transactions of the Royal Society of London A: Mathematical, Physical and Engineering Sciences, 363, 1677–1700, 2005.

Herman, A., Evers, K.-U., and Reimer, N.: Floe-size distributions in laboratory ice broken by waves, The Cryosphere, 12, 685–699, 2018.

Hibler III, W. D.: A Dynamic Thermodynamic Sea Ice Model, Journal of Physical Oceanography, 9, 815–846, https://doi.org/10.1175/1520-0485(1979)009<0815:ADTSIM>2.0.CO;2, 1979.

Horvat, C. and Tziperman, E.: A prognostic model of the sea-ice floe size and thickness distribution, The Cryosphere, 9, 2119–2134, https://doi.org/10.5194/tc-9-2119-2015, http://www.the-cryosphere.net/9/2119/2015/, 2015.

Hunke, E. C. and Dukowicz, J. K.: An Elastic–Viscous–Plastic Model for Sea Ice Dynamics, Journal of Physical Oceanography, 27, 1849–1867, https://doi.org/10.1175/1520-0485(1997)027<1849:AEVPMF>2.0.CO;2, 1997.

Inoue, J., Wakatsuchi, M., and Fujiyoshi, Y.: Ice floe distribution in the Sea of Okhotsk in the period when sea-ice extent is advancing, Geophysical research letters, 31, 2004.

Jackson, J., Carmack, E., McLaughlin, F., Allen, S. E., and Ingram, R.: Identification, characterization, and change of the near-surface temperature maximum in the Canada Basin, 1993–2008, Journal of Geophysical Research: Oceans, 115, 2010.

Khon, V., Mokhov, I., Pogarskiy, F., Babanin, A., Dethloff, K., Rinke, A., and Matthes, H.: Wave heights in the 21st century Arctic Ocean simulated with a regional climate model, Geophysical Research Letters, 41, 2956–2961, 2014.

Kohout, A. L., Williams, M. J. M., Dean, S. M., and Meylan, M. H.: Storm-induced sea-ice breakup and the implications for ice extent, Nature, 509, 604–607, https://doi.org/10.1038/nature13262, 2014.

Langhorne, P. J., Squire, V. A., Fox, C., and Haskell, T. G.: Break-up of sea ice by ocean waves, Annals of Glaciology, 27, 438–442, 1998.

Lee, C. M., Cole, S., Doble, M., Freitag, L., Hwang, P., Jayne, S., Jeffries, M., Krishfield, R., Maksym, T., and Maslowski, W.: Marginal Ice Zone (MIZ) program: Science and experiment plan, Tech. rep., WASHINGTON UNIV SEATTLE APPLIED PHYSICS LAB, 2012.

Lemieux, J.-F., Lei, J., Dupont, F., Roy, F., Losch, M., Lique, C., and Laliberté, F.: The Impact of Tides on Simulated Landfast Ice in a Pan-Arctic Ice-Ocean Model, Journal of Geophysical Research: Oceans, 123, 7747–7762, 2018.

Lique, C., Holland, M. M., Dibike, Y. B., Lawrence, D. M., and Screen, J. A.: Modeling the Arctic freshwater system and its integration in the global system: Lessons learned and future challenges, Journal of Geophysical Research: Biogeosciences, 121, 540–566, 2016.

Longuet-Higgins, M. S.: The mean forces exerted by waves on floating or submerged bodies with applications to sand bars and wave power machines, Proc. Roy. Soc. Lond. A, 352, 463–480, 1977.

Longuet-Higgins, M. S. and Stewart, R. W.: Radiation stresses and mass transport in surface gravity waves with application to 'surf beats', J. Fluid Mech., 13, 481–504, 1962.

Lüpkes, C., Gryanik, V. M., Hartmann, J., and Andreas, E. L.: A parametrization, based on sea ice morphology, of the neutral atmospheric drag coefficients for weather prediction and climate models, Journal of Geophysical Research: Atmospheres, 117, 2012.

Madec, G.: NEMO ocean engine, Note du Pôle de modélisation, Institut Pierre-Simon Laplace (IPSL), France, No 27, ISSN No 1288-1619, 2008.

Marcq, S. and Weiss, J.: Influence of sea ice lead-width distribution on turbulent heat transfer between the ocean and the atmosphere, The Cryosphere, 6, 143–156, 2012.

Martin, S. and Kauffman, P.: A Field and Laboratory Study of Wave Damping by Grease Ice, Journal of Glaciology, 27, 283–313, https://doi.org/10.1017/S0022143000015392, 1981.

Maykut, G. A. and Perovich, D. K.: The role of shortwave radiation in the summer decay of a sea ice cover, Journal of Geophysical Research: Oceans, 92, 7032–7044, 1987.

McPhee, M. G.: An analysis of pack ice drift in summer, Sea ice processes and models, pp. 62–75, 1980.

Mellor, M.: Mechanical Behavior of Sea Ice, in: The Geophysics of Sea Ice, edited by Untersteiner, N., NATO ASI Series, pp. 165–281, Springer US, https://doi.org/10.1007/978-1-4899-5352-0_3, 1986.

Montiel, F., Squire, V. A., and Bennetts, L. G.: Attenuation and directional spreading of ocean wave spectra in the marginal ice zone, J. Fluid Mech., 790, 492–522, https://doi.org/10.1017/jfm.2016.2, 2016.

Perrie, W. and Hu, Y.: Air–ice–ocean momentum exchange. Part II: Ice drift, Journal of physical oceanography, 27, 1976–1996, 1997.

Rainville, L., Lee, C. M., and Woodgate, R. A.: Impact of wind-driven mixing in the Arctic Ocean, Oceanography, 24, 136–145, 2011.

Rampal, P., Bouillon, S., Olason, E., and Morlighem, M.: neXtSIM: a new Lagrangian sea ice model, CRYOSPHERE, 10, https://doi.org/10.5194/tc-10-1055-2016, 2016.

Roach, L. A., Horvat, C., Dean, S. M., and Bitz, C. M.: An emergent sea ice floe size distribution in a global coupled ocean–sea ice model, Journal of Geophysical Research: Oceans, 2018.

Rogers, W. E., Thomson, J., Shen, H. H., Doble, M. J., Wadhams, P., and Cheng, S.: Dissipation of wind waves by pancake and frazil ice in the autumn Beaufort Sea, J. Geophys. Res., 121, https://doi.org/10.1002/2016JC012251, 2016.

Rothrock, D. and Thorndike, A.: Measuring the sea ice floe size distribution, Journal of Geophysical Research: Oceans, 89, 6477–6486, 1984.

Rousset, C., Vancoppenolle, M., Madec, G., Fichefet, T., Flavoni, S., Barthélemy, A., Benshila, R., Chanut, J., Lévy, C., Masson, S., et al.: The Louvain-La-Neuve sea ice model LIM3. 6: global and regional capabilities, Geoscientific Model Development, 8, 2991, 2015.

Shen, H. H. and Ackley, S. F.: A one-dimensional model for wave-induced ice-floe collisions, Annals of Glaciology, 15, 87–95, 1991.

Smith, M., Stammerjohn, S., Persson, O., Rainville, L., Liu, G., Perrie, W., Robertson, R., Jackson, J., and Thomson, J.: Episodic reversal of autumn ice advance caused by release of ocean heat in the Beaufort Sea, Journal of Geophysical Research: Oceans, 2018.

Squire, V. A.: A fresh look at how ocean waves and sea ice interact, Phil. Trans. R. Soc. A, 376, 20170 342, 2018.

Steele, K., Teng, C.-C., and Wang, D. W.-C.: Wave direction measurements using pitch and roll buoys, Ocean Eng., 19, 349–375, 1992.

Steele, M.: Sea ice melting and floe geometry in a simple ice-ocean model, Journal of Geophysical Research: Oceans, 97, 17 729–17 738, https://doi.org/10.1029/92JC01755, 1992.

Steele, M., Morison, J. H., and Untersteiner, N.: The partition of air-ice-ocean momentum exchange as a function of ice concentration, floe size, and draft, Journal of Geophysical Research: Oceans, 94, 12 739–12 750, 1989.

Stopa, J., Ardhuin, F., Thomson, J., Smith, M. M., Kohout, A., Doble, M., and Wadhams, P.: Wave Attenuation Through an Arctic Marginal Ice Zone on 12 October, 2015: 1. Measurement of Wave Spectra and Ice Features From Sentinel-1A, Journal of Geophysical Research: Oceans, 2018a.

Stopa, J. E., Ardhuin, F., and Girard-Ardhuin, F.: Wave climate in the Arctic 1992-2014: seasonality and trends, The Cryosphere, 10, 1605–1629, https://doi.org/10.5194/tc-10-1605-2016, 2016a.

Stopa, J. E., Ardhuin, F., Husson, R., Jiang, H., Chapron, B., and Collard, F.: Swell dissipation from 10 years of Envisat ASAR in wave mode, Geophys. Res. Lett., 43, 3423–3430, https://doi.org/10.1002/2015GL067566, 2016b.

Stopa, J. E., Sutherland, P., and Ardhuin, F.: Strong and highly variable push of ocean waves on Southern Ocean sea ice, Proceedings of the National Academy of Sciences, 115, 5861–5865, 2018b.

Stroeve, J., Hamilton, L. C., Bitz, C. M., and Blanchard-Wrigglesworth, E.: Predicting September sea ice: Ensemble skill of the SEARCH Sea Ice Outlook 2008-2013, Geophys. Res. Lett., 41, 2411–2418, https://doi.org/10.1002/2014GL059388, 2014.

Strong, C. and Rigor, I. G.: Arctic marginal ice zone trending wider in summer and narrower in winter, Geophysical Research Letters, 40, 4864–4868, https://doi.org/10.1002/grl.50928, 2013.

Sutherland, P. and Dumont, D.: Marginal ice zone thickness and extent due to wave radiation stress., Journal of Physical Oceanography, 2018.

Sutherland, P. and Melville, W. K.: Field measurements and scaling of ocean surface wave-breaking statistics, Geophys. Res. Lett., 40, 3074–3079, https://doi.org/10.1002/grl.50584, 2013.

The WAVEWATCH III® Development Group: User manual and system documentation of WAVEWATCH III ® version 5.16, Tech. Note 329, NOAA/NWS/NCEP/MMAB, College Park, MD, USA, 326 pp. + Appendices, 2016.

Thomson, J. and Rogers, W. E.: Swell and sea in the emerging Arctic Ocean, Geophys. Res. Lett., 41, 3136–3140, https://doi.org/10.1002/2014GL059983, 2014.

Thomson, J., Ackley, S., Girard-Ardhuin, F., Ardhuin, F., Babanin, A., Bidlot, J., Boutin, G., Brozena, J., Cheng, S., Doble, M., et al.: Overview of the arctic sea state and boundary layer physics program, Journal of Geophysical Research: Oceans, 2018.

Timmermans, M.-L.: The impact of stored solar heat on Arctic sea ice growth, Geophysical Research Letters, 42, 6399–6406, 2015.

Toyota, T., Haas, C., and Tamura, T.: Size distribution and shape properties of relatively small sea-ice floes in the Antarctic marginal ice zone in late winter, Deep Sea Research Part II: Topical Studies in Oceanography, 58, 1182–1193, 2011.

Uotila, P., Goosse, H., Haines, K., Chevallier, M., Barthélemy, A., Bricaud, C., Carton, J., Fučkar, N., Garric, G., Iovino, D., et al.: An assessment of ten ocean reanalyses in the polar regions, Climate Dynamics, pp. 1–38, 2018.

Vancoppenolle, M., Fichefet, T., Goosse, H., Bouillon, S., Madec, G., and Maqueda, M. A. M.: Simulating the mass balance and salinity of Arctic and Antarctic sea ice. 1. Model description and validation, Ocean Modelling, 27, 33–53, 2009.

Wang, Q., Ilicak, M., Gerdes, R., Drange, H., Aksenov, Y., Bailey, D. A., Bentsen, M., Biastoch, A., Bozec, A., Böning, C., et al.: An assessment of the Arctic Ocean in a suite of interannual CORE-II simulations. Part II: Liquid freshwater, Ocean Modelling, 99, 86–109, 2016.

Waseda, T., Webb, A., Sato, K., Inoue, J., Kohout, A., Penrose, B., and Penrose, S.: Correlated Increase of High Ocean Waves and Winds in the Ice-Free Waters of the Arctic Ocean, Scientific Reports, 8, 4489, https://doi.org/10.1038/s41598-018-22500-9, https://doi.org/10.1038/s41598-018-22500-9, 2018.

Williams, T. D., Bennetts, L. G., Squire, V. A., Dumont, D., and Bertino, L.: Wave-ice interactions in the marginal ice zone. Part 2: Numerical implementation and sensitivity studies along 1D transects of the ocean surface, Ocean Modelling, 71, 92–101, https://doi.org/10.1016/j.ocemod.2013.05.011, 2013.

Williams, T. D., Rampal, P., and Bouillon, S.: Wave-ice interactions in the neXtSIM sea-ice model, The Cryosphere Discussions, pp. 1–28, https://doi.org/10.5194/tc-2017-24, 2017.

Zhang, J., Schweiger, A., Steele, M., and Stern, H.: Sea ice floe size distribution in the marginal ice zone: Theory and numerical experiments: Modeling floe size distribution, Journal of Geophysical Research: Oceans, 120, 3484–3498, https://doi.org/10.1002/2015JC010770, 2015.

Zhang, J., Stern, H., Hwang, B., Schweiger, A., Steele, M., Stark, M., and Graber, H. C.: Modeling the seasonal evolution of the Arctic sea ice floe size distribution, Elementa, 4, https://doi.org/10.12952/journal.elementa.000126, 2016.

Zhao, J., Barber, D., Zhang, S., Yang, Q., Wang, X., and Xie, H.: Record low sea-ice concentration in the central Arctic during summer 2010, Advances in Atmospheric Sciences, 35, 106–115, 2018.

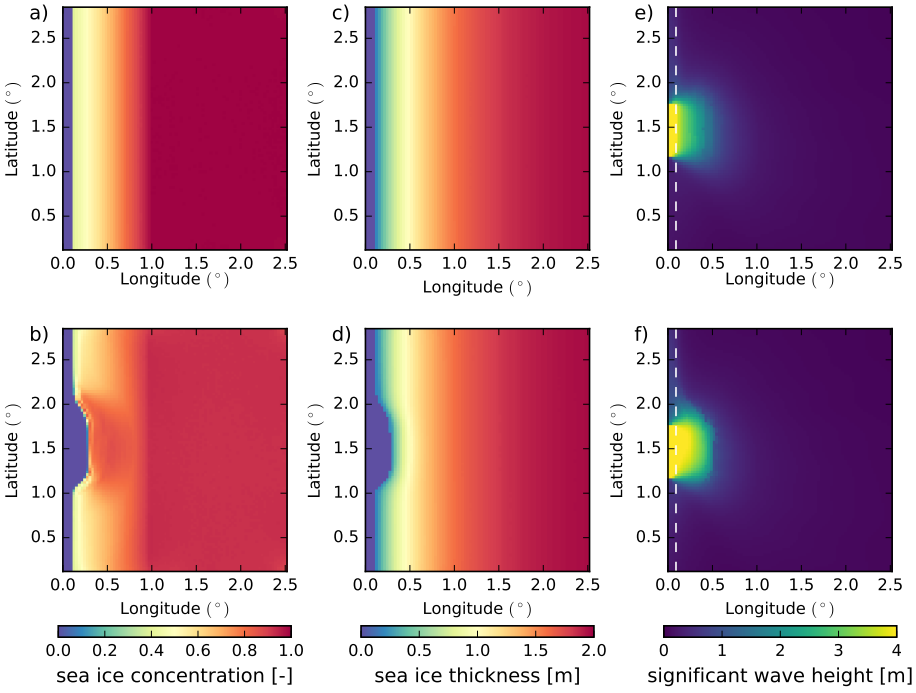

Figure 1. Implementation of the WRS in the idealized configuration. (a) and (c) show the initial state of sea ice concentration and thickness (ice-cover average), respectively. (b) and (d) show sea ice concentration and thickness after 72 h in the WW3-LIM3 coupled model. (e) and (f) show the significant wave height Hs distribution after 72 h in the WW3 model and in the WW3-LIM3 coupled model, respectively. The white dashed line on (e) and (f) indicates the position of the ice edge (c=0.15).

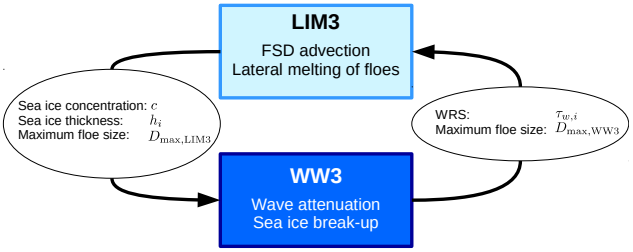

Figure 2. Schematic ~~summarizing~~ summary of the exchanged information between the sea ice model LIM3 and the wave model WAVEWATCH III® in our coupled framework. The two boxes ~~corresponds~~ correspond to the processes accounted for in a given model, while the variables exchanged between the models are listed in the bubbles.

.

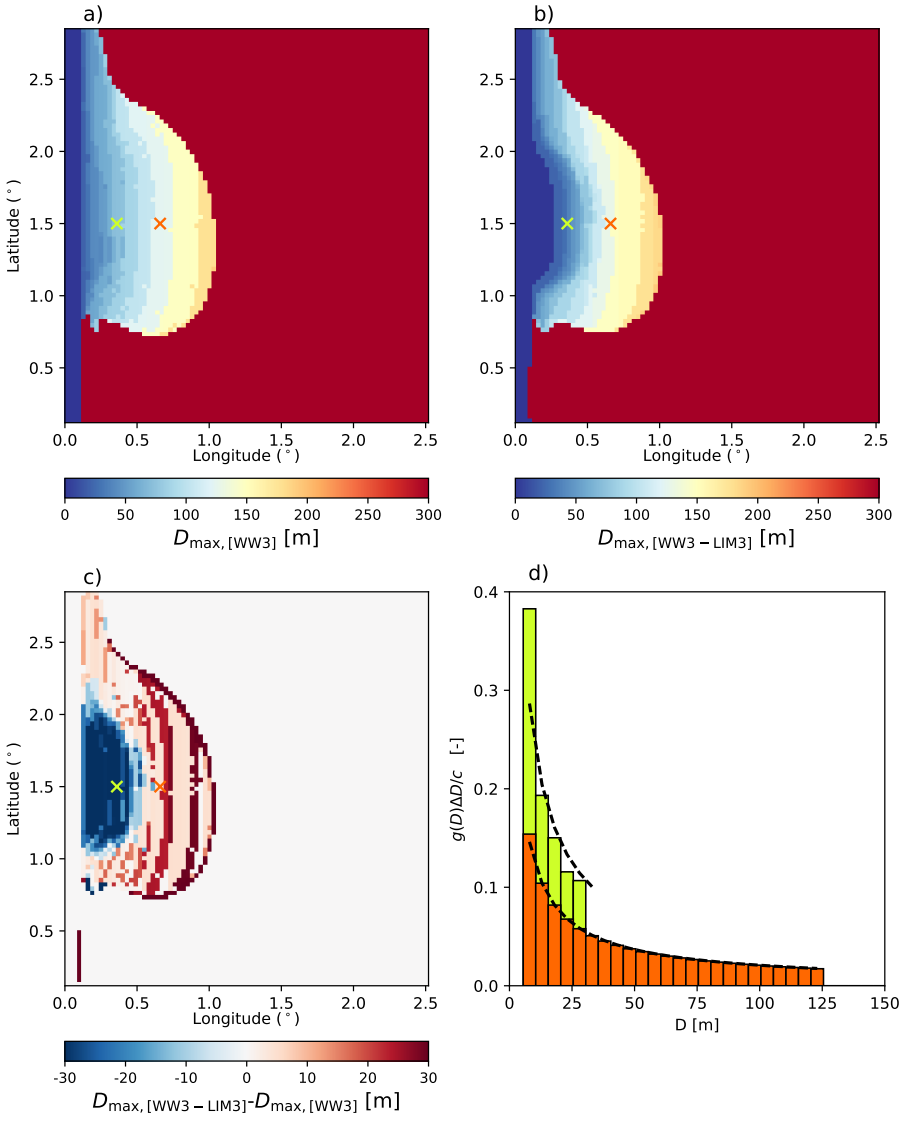

Figure 3. Snapshots of $D_{\max}$ from the uncoupled WW3 (a) and the WW3-LIM3 (b) simulations after 72 h, and the difference between the two (c). Panel (d) shows the FSD from the WW3-LIM3 run at two locations indicated with crosses on panels a,b,c. The black dashed line in (d) corresponds to the theoretical power-law FSD assumed in WW3.

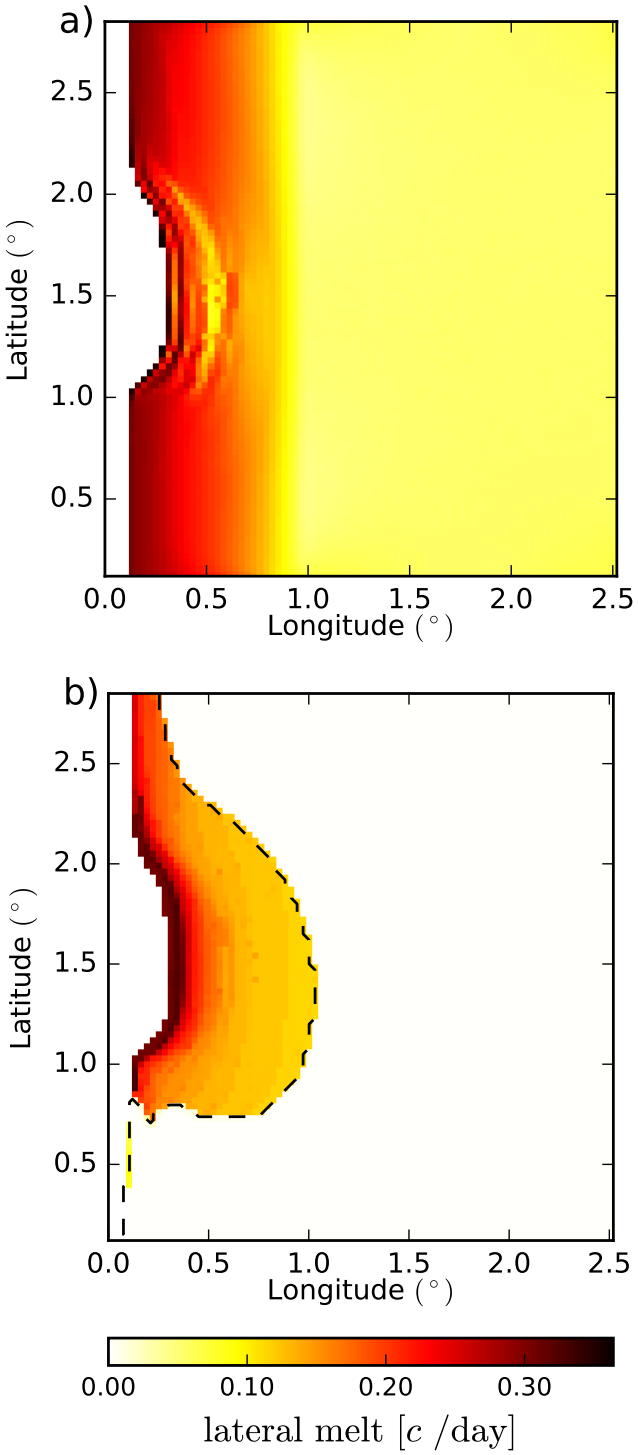

Figure 4. Lateral melt rates [estimated as percentage of sea ice concentration lost per day] estimated by the coupled model after 72 h of simulation using the parameterization of Lüpkes et al. (2012) (a), or the parameterization developed in this study accounting for wave-induced sea ice ~~break up~~ fragmentation (b). The black dashed contour on panel (b) indicates $D_{\max} = 500\ m$, and thus represents the limit between broken and unbroken sea ice.

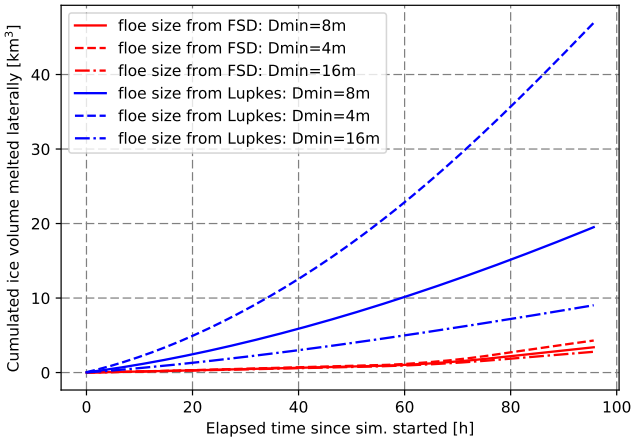

Figure 5. Temporal evolution of the sea ice volume loss due to lateral melt integrated over the whole domain for simulations similar to the one presented in Fig. 4, but for different values of $D_{\min}$. The two colors correspond to the two lateral melt parameterizations used in this study.

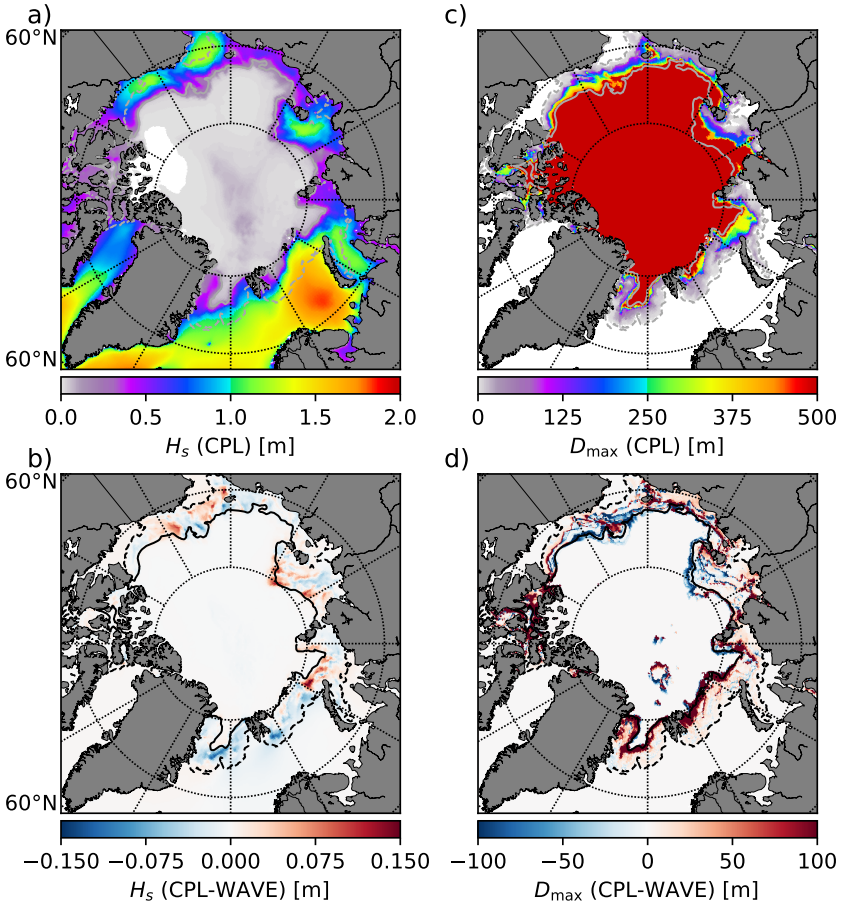

Figure 6. Significant wave height (a) and maximum floe size (c) in the CPL simulation averaged over the period 03-08-2010 to 09-09-2018, and the differences with the WAVE simulations (b, d). The black and grey contours delimit the MIZ in the CPL simulation, defined here as $0 < \langle D_{\max} \rangle < 700$ m. Note that the sea ice conditions from the NOT_CPL run are used as forcing for the WAVE run and are thus similar in the WAVE and the NOT_CPL runs.

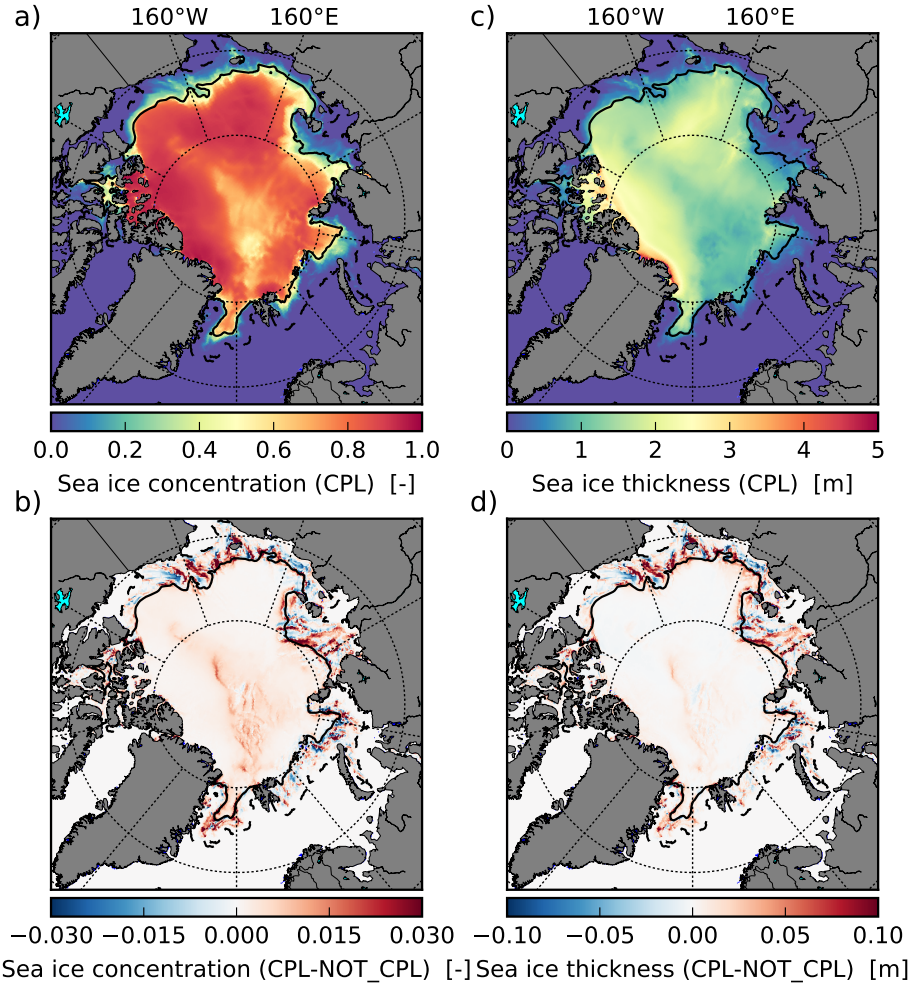

Figure 7. Sea ice concentration and thickness in the CPL simulation (a, c) and the difference with NOT_CPL (b,d) averaged over the period 04/08/2010 to 09/09/2010. The black contours delimit the MIZ in the CPL simulation, defined here as $0 < \langle D_{\max} \rangle < 700$ m.

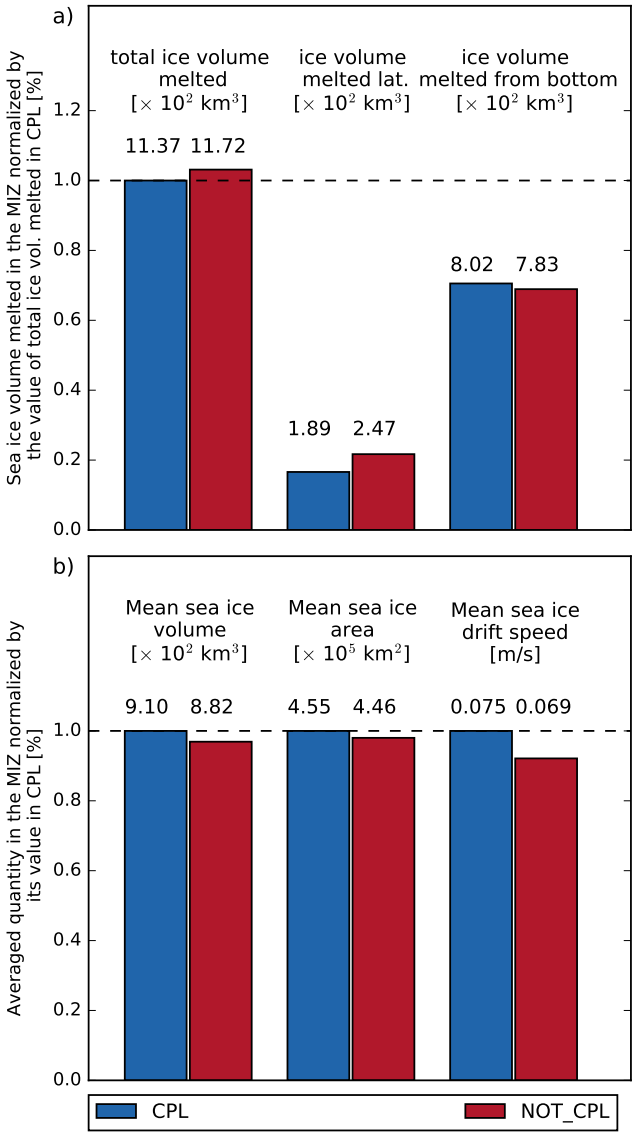

Figure 8. (a) Sea ice volume melted (in 10^2km^3) integrated over the MIZ and over the period between 04/08/2010 and 09/09/2010 in the CPL and the NOT_CPL simulations. Here the MIZ is defined as the region where $0 < \langle D_{\max} \rangle < 700$ m in the CPL run. The contribution from lateral melt and bottom melt to the total melt for both simulations are also represented. (b) Mean sea ice volume (in 10^2km^3), area (in 10^5km^2), and drift speed (in m/s) in the MIZ over the same period. Values for each simulation are found above their associated bar.

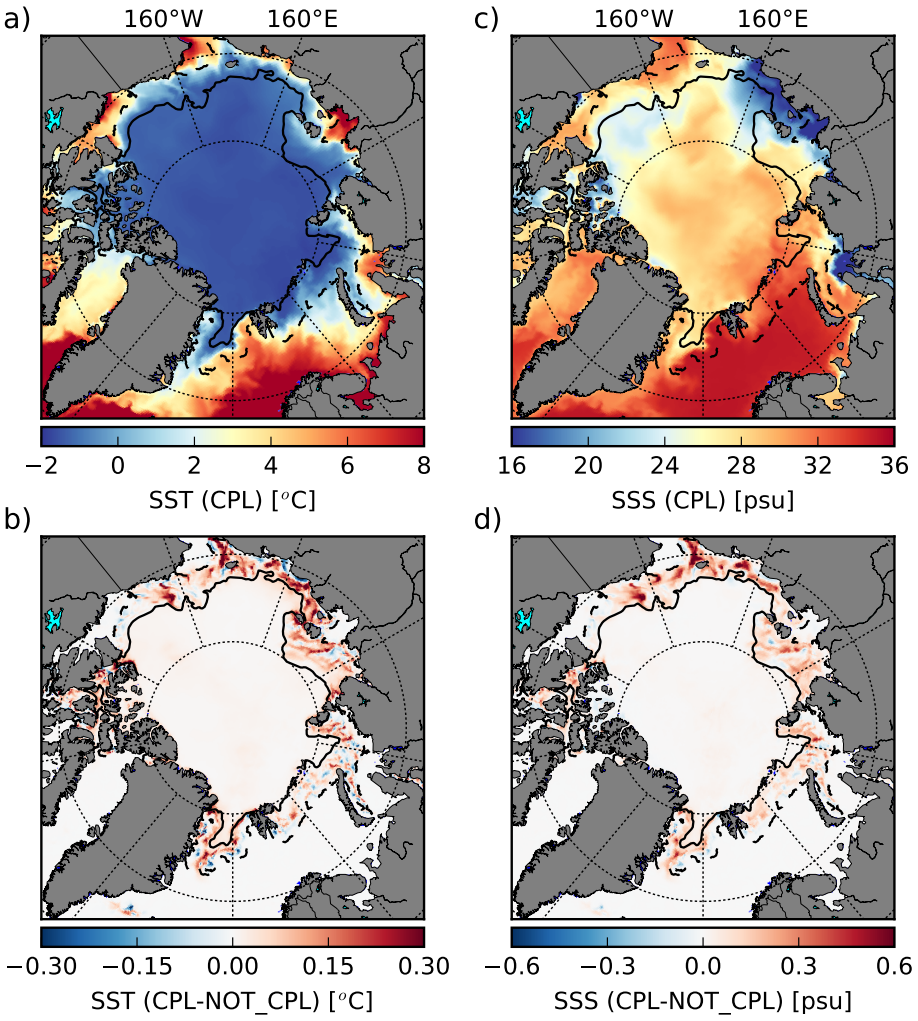

Figure 9. SST (a) and SSS (c) in the CPL run for the period between between 04/08/2010 and 09/09/2010, and the difference with NOT_CPL (b,d). The black contours delimit the MIZ in the CPL simulation, defined here as $0 < \langle D_{\max} \rangle < 700$ m.

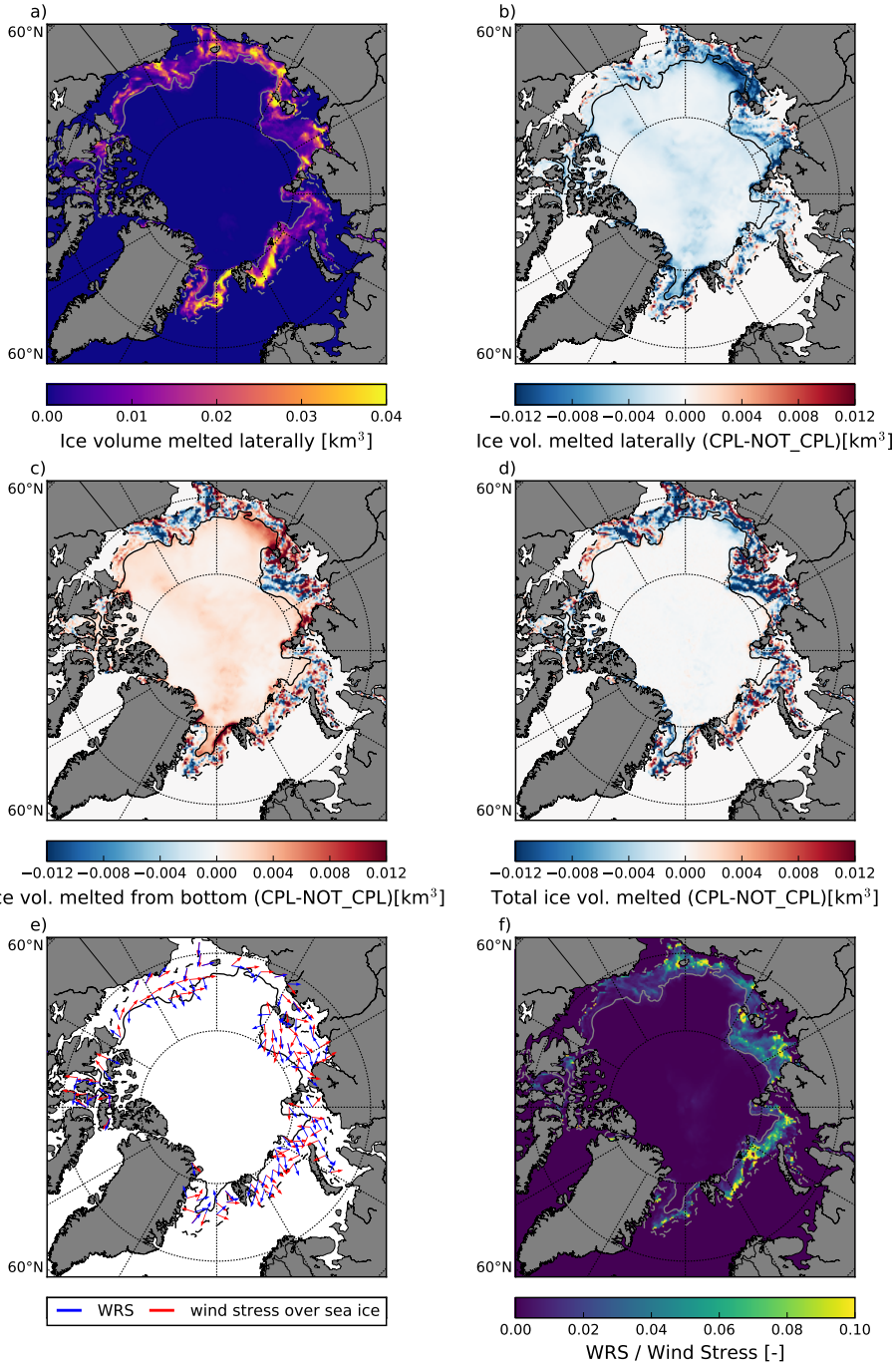

Figure 10. Volume of sea ice melted by lateral melt in the CPL simulation over the period between 04/08/2010 and 09/09/2010 (a). Differences between the CPL and the NOT_CPL runs of lateral melt (b), bottom melt (c) and total melt (d). (e) Wind stress (red) and WRS (blue) averaged over the same period 04/08/2010 and 09/09/2010 in the CPL simulation. Note that the WRS has been multiplied by a factor of 10 in order to improve readability. (f) Distribution of the relative magnitude of WRS over the wind stress. The grey contours represent the position of the ice edge ($c = 0.15$) on the first (solid line) and last day (dashed line) of the period considered in the CPL simulation.

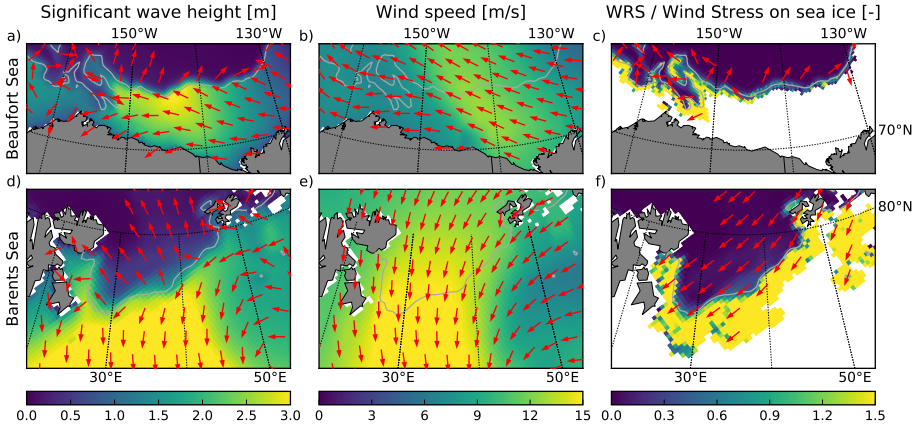

Figure 11. Significant wave height and wave mean direction of propagation (a, d), wind speed (b, e) and WRS (c, f) simulated by the CPL run during the storms that occurred in the Beaufort Sea (a, b, c) and in the Barents Sea (d, e, f) on 16/08/2010-17/08/2010. The grey contours indicate the position of the sea ice edge determined from the averaged sea ice concentration ($c = 0.15$).

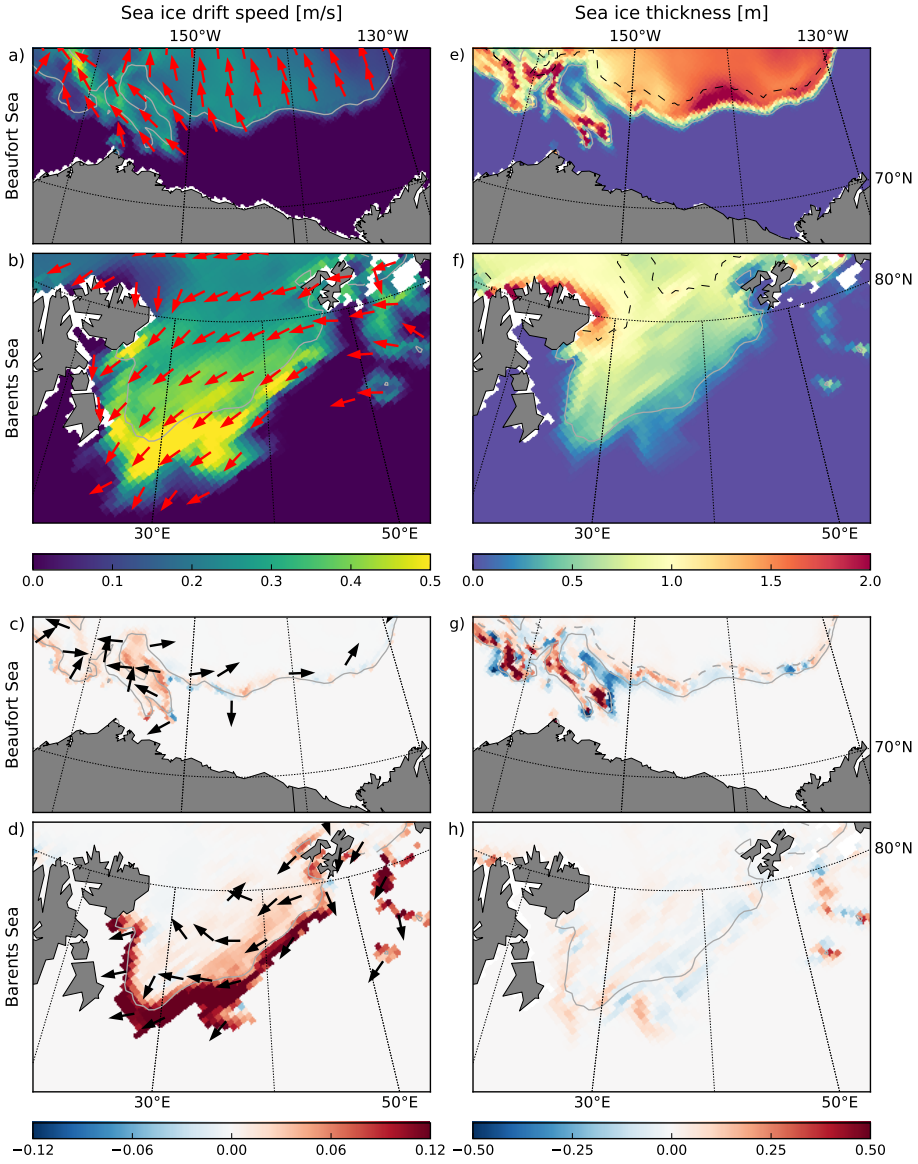

Figure 12. Mean sea ice drift (a, b) and sea ice thickness (e, f) simulated by the CPL run during the storms that occurred in the Beaufort Sea (a, c) and in the Barents Sea (b, f) on 16/08/2010-17/08/2010. Panels (c, d, g, h) show the differences for these quantities between the CPL and NOT_CPL simulations. Grey contours indicate the position of the ice edge determined from the averaged sea ice concentration ($c = 0.15$). The black dashed contour delimits the border between broken and unbroken ice ($D_{\max} = 500$m)

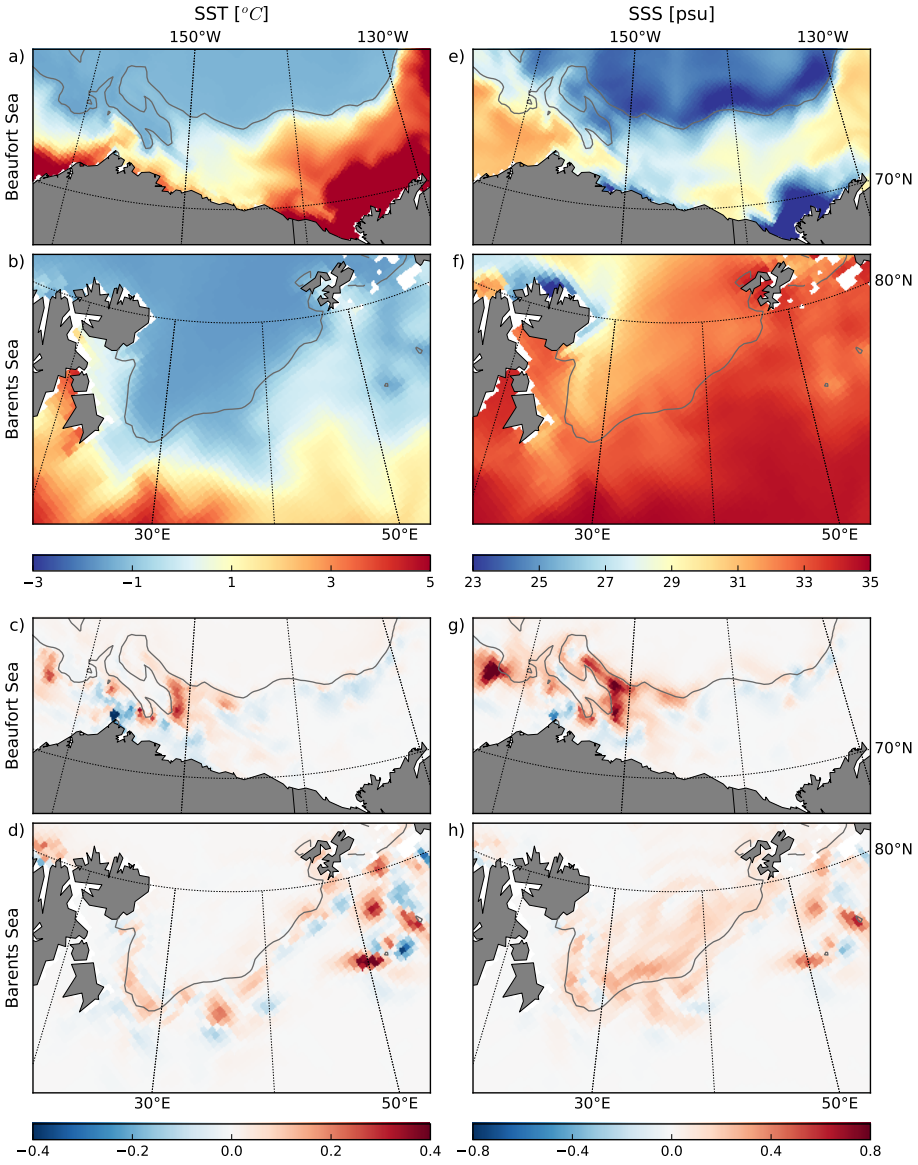

Figure 13. SST (a, b) and SSS (e, f) simulated by the CPL run during the storms that occurred in the Beaufort Sea (a, c) and in the Barents Sea (b, f) on 16/08/2010-17/08/2010. Panels (c, d, g, h) show the differences for these quantities between the CPL and NOT_CPL simulations. Grey contours indicate the position of the ice edge determined from the averaged sea ice concentration ($c = 0.15$).

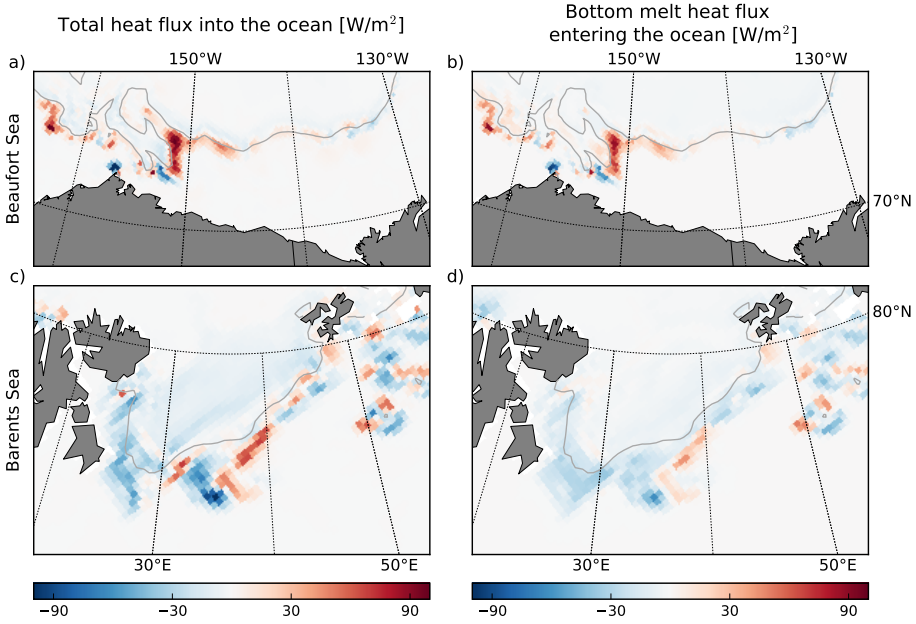

Figure 14. Averaged differences between the CPL and NOT_CPL simulations of (a, c) the heat flux into the ocean and (b, d) the contribution to the heat flux into the ocean coming from the sea ice bottom melt during the storms in the Beaufort Sea (a, b) and in the Barents Sea (c, d) which occurred on 16/08/2010-17/08/2010. Grey contours indicate the position of the ice edge determined from the averaged sea ice concentration ($c = 0.15$).